

Recent Advances in Hollow Nanostructures: Synthesis Methods, Structural Characteristics, and Applications in Food and Biomedicine

Yajuan Li, Jingbo Liu, David Julian McClements, Xin Zhang, Ting Zhang, and Zhiyang Du*



Cite This: *J. Agric. Food Chem.* 2024, 72, 20241–20260



Read Online

ACCESS |

Metrics & More

Article Recommendations

ABSTRACT: The development and investigation of innovative nanomaterials stand poised to advance technological progress and meet the contemporary demand for efficient, environmentally friendly, and intelligent products. Hollow nanostructures (HNS), characterized by their hollow architecture, exhibit diverse properties such as expansive specific surface area, low density, high drug-carrying capacity, and customizable structures. These elaborated structures, encompass nanospheres, nanoboxes, rings, cubes, and nanowires, have wide-ranging applications in biomedicine, materials chemistry, food industry, and environmental science. Herein, HNS and their cutting-edge synthesis methods, including solvothermal methods, liquid-interface assembly methods, and the self-templating methods are discussed in-depth. Meanwhile, the potential applications of HNS in food and biomedicine such as food packing, biosensor, and drug delivery over the past three years are summarized, together with a prospective view of future research directions and challenges. This review will offer new insights into designing next generation of hollow nanomaterials for food and biomedicine applications.

KEYWORDS: hollow nanostructure, nanomaterials, food packing, biosensor, drug delivery

1. INTRODUCTION

Since the Industrial Revolution, human society has witnessed unprecedented development, propelled by scientific and technological advancements and the surge of industrialization, leading to significant economic growth. Nonetheless, the accelerated pace of globalization and the deepening of industrialization have brought issues such as food safety, environmental pollution, and health risks a global concern.^{1,2} In addressing these challenges, the research, development, and application of novel materials have become paramount. The rapid advancement of nanotechnology offers a promising platform for the generation of green and health-promoting new materials.^{3,4} Scientists have innovated a variety of functional nanomaterials characterized by diverse structures, utilizing biodegradable, biocompatible, and biosafe raw materials such as proteins, polysaccharides, liposomes, and metal–organic frameworks. These nanomaterials, encompassing nanospheres, nanotubes, fibers, and hollow structures, which can be widely implemented in biomedicine,⁵ materials chemistry,⁶ environmental science,⁷ and food industry.^{8,9} Among these novel nanostructures, hollow nanostructures (HNS) are particularly distinguished due to their unique architectures and exceptional physicochemical properties.

HNS are nanoscale entities with hollow architecture, usually consisting of an outer shell and an inner cavity.¹⁰ The shell material can be metals, metal oxides, polymers, or other substance.¹¹ Table 1 summarized the advantages and disadvantages of the various shell materials commonly used for synthetic hollow structures. Since the pioneering work of Caruso and colleagues in 1998 in synthesizing hybrid spheres

of hollow silica and inorganic-polymer,¹² a plethora of inorganic and organic hollow structures have been meticulously investigated (Figure 1). Their morphology has transcended the traditional spherical shape to encompass ellipsoids, nanoboxes, rods, rings, cubes, nanowires, and more (Figure 2).^{10,13} Simultaneously, methods for synthesizing hollow structures have transitioned from the traditional approaches¹⁰ such as the hard template method and soft template method to more innovative methods, including solvothermal methods, liquid-interface assembly methods, and the self-templating methods, among others.¹¹ More importantly, compared to solid structures, hollow structures possess a range of captivating properties, including a large specific surface area, low density, high drug-carrying capacity, and tunable architecture.¹⁴ With these properties, new functional materials can be rationally designed to meet the needs of multiple applications. Initially, HNS were primarily employed in electrochemistry^{15,16} (e.g., battery electrode materials and electrochemical sensor) and energy storage^{17,18} (including supercapacitors and hydrogen storage material). Over time, research advancements have broadened the scope of hollow nanostructures' applications to encompass sectors

Received: July 3, 2024

Revised: August 20, 2024

Accepted: August 30, 2024

Published: September 10, 2024

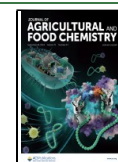
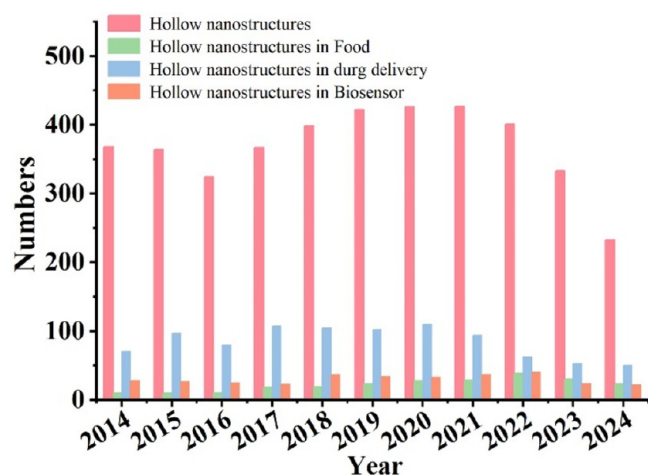


Table 1. Advantages and Disadvantages of Various Shell Materials Used in Hollow Nanostructures

| shell materials | advantages | disadvantages |
|---|---|---|
| metals (e.g., Au, Ag, Pt) | -high conductivity -catalytic activity -stability | -high cost -toxicity -heavy weight |
| metal oxides (e.g., TiO ₂ , SiO ₂) | -photocatalytic properties -biocompatibility -high chemical and thermal stability -functionalizability | -fragility -lower conductivity -complex synthesis |
| carbon-based materials (e.g., graphene, carbon nanotubes) | -high electrical conductivity -excellent mechanical strength -versatility and functionalizability -high surface area | -complex production -potential toxicity -aggregation |
| polymers | -flexible and responsive to stimuli -biodegradability -easy to functionalize -low cost | -lower mechanical strength -thermal sensitivity -potential toxicity |
| hybrid materials (e.g., metal–polymer composites) | -tailored properties -enhanced functionality -versatility | -complex synthesis -incompatibility issue -high cost |

**Figure 1.** Number of published articles related to hollow nanostructures and hollow nanostructures applied to the fields of food, drug delivery, and biosensors (searched on Web of Science and PubMed with the following keyword: “Hollow Nanostructure,” “Hollow Nanostructure in Food,” “Hollow Nanostructure in Drug Delivery,” and “Hollow Nanostructure in Biosensor” from 2014 to June 2024).

like the food industry and environmental agriculture, drug delivery, and biosensors (Figure 1).^{5,7,19} For instance, hollow nanoparticles (NPs) offer a promising avenue for developing

**Figure 2.** Schematic illustration showing various hollow structures.

sustainable food packaging materials, owing to their exceptional barrier and antimicrobial properties.²⁰ Integrating hollow NPs into packaging materials enhances their barrier capabilities against oxygen, water vapor, and other gases, thereby extending the shelf life of food products.^{20–22} Moreover, these NPs can be loaded with antimicrobial agents and released gradually, thereby inhibiting microbial growth and enhancing food safety.^{23,24} In addition, the large specific surface area and facile surface modification of HNS make it possible to fabricate biosensors with high sensitivity and selectivity.^{25,26} Such biosensors can utilize the unique properties of the hollow structure to detect hazardous substances such as pesticide residues,²⁷ hydrazine,²⁸ and microbial contaminants²⁹ in food products with rapid response times and high detection limits.³⁰ In the realm of functional foods and nutritional supplements, HNS could serve as effective carriers for delivering vitamins, antioxidants, and other bioactive compounds.^{31–33}

Recently, there has been a growing number of reviews on the synthesis of HNS materials and their applications in energy storage, conversion, and electrochemistry.^{5,10,11,19,34} However, comprehensive reviews on the emerging structures, synthesis methods, and applications of HNS in the food industry over the past three years are virtually nonexistent. In this review, we commence by exploring the distinctive hollow structures that have emerged in the past three years. Additionally, we delve into recent strategies for synthesizing these HNS. Finally, we provide a synthesis of their current and potential applications in the realm of food science and medicine, alongside an outlook on future research directions and challenges.

2. STRUCTURE AND MORPHOLOGY OF HNS

The structure and morphology of HNS are pivotal in determining their functionality. Over time, their configurations have evolved from basic single-layer spherical forms to more intricate designs such as hollow fibers, rings, yolk–shell architectures, and multilayered spherical shells (Figure 2). This section will take an in-depth look at hollow NPs of

various shapes and structures synthesized in the last three years, focusing on their sophistication and complexity

2.1. Hollow Nanofibers. Hollow nanofibers are a type of nanofiber morphology characterized by a central hollow space, which is uniquely advantageous in the field of electrochemical energy storage due to their large surface area and engineered high porosity.³⁵ In general, the outer surface of hollow nanofiber structures is usually modified by some small-sized secondary structures such as NPs, nanosheets, and nanopins to form multistructured nanofibers.³⁶ For example, hollow carbon fibers modified by atomic Fe–N₄ and encapsulated with Ni NPs (Fe–N@Ni–HCFs) exhibit a unique lung bubble-like hollow structure (Figure 3A).¹⁶ MoS₂-modified bow-shaped

hollow fibers with abundant heterogeneous interfaces (Figure 3D).³⁹ Wang et al. developed a range of multifunctional nanodoped hollow fibers by incorporating various materials into hollow fibers hydrogel.⁴⁰

In addition to surface modifications, the internal structure of the fibers can also be altered to form hollow nanofibers with complex internal architectures, such as multiwalled, multi-channel, and porous structures. For example, Gao and his team synthesized a hierarchical hollow nanofiber (MoO₃@NiO) using molybdenum disulfide (MoS₂) and NiS_{1.03}-C, where NiS_{1.03}-C forms a pea-pod-like shell, encapsulating MoS₂ NPs like beans (Figure 3E).⁴¹ Besides, Fe₃C was employed to embellish N-doped hollow carbon nanofibers (HMCs), yielding porous composite carbon nanofibers with intrinsic hollow structures (Figure 3F).⁴² The “tube-in-fiber” structure have been meticulously designed by confining carbon nanotubes (CNTs) within Co-doped hollow multichannel carbon fibers (MCCFs-Co), serving as the sulfur host material for lithium–sulfur batteries (Figure 3G).⁴³ He et al. developed innovative porous membrane structures (Fiber/HNTs/ZIF-67) using hollow wood fibers as the backbone, with halloysite nanotubes and metal–organic framework NPs (ZIF-67) as filler material, which exhibited excellent thermal stability and mechanical properties (Figure 3H).⁴⁴ Shin et al. employed a dual-nozzle electrospinning technique to successfully fabricate free-standing, porous, hollow carbon nanofibers (HCNF) embedded with lithiophilic ZnO NPs (Figure 3I).⁴⁵ Among the various types of multistage hollow nanofibers, surface modification has been more extensively studied, while fewer investigations have focused on nanofibers with complex internal architectures. This discrepancy arises because modulating the internal structure within a confined space is more challenging than altering the external morphology, and the mechanism behind the formation of hierarchical hollow structures remains poorly understood. Consequently, the construction of multiscale hollow nanofiber structures and the elucidation of their formation mechanisms require further in-depth research.

2.2. Yolk–Shell Structures. The yolk–shell structure is a type of core–shell architecture where the core is detached from the shell and consists of a single movable core material within a hollow shell, with a void region between the core and shell.¹⁵ Yolk–shell structures have profoundly impacted the field of metal nanomaterials research and have been investigated with an array of shells composed of diverse materials. However, the evolution of zeolite-based yolk–shell structures has predominantly adhered to conventional design approaches, lacking in innovative breakthroughs.⁴⁶ In recent years, some avant-garde design concepts have emerged, aiming to produce nanomaterials with yolk–shell architectures that exhibit enhanced innovation and functionality.

For example, Liu et al. engineered yolk–shelled CoS₂@FeS₂@NC hollow microspheres through a meticulous step-by-step process. Initially, a Co-G microsphere precursor was synthesized. Subsequently, Fe-G nanosheets were methodically grown on the surface of the Co-G microspheres via a solvothermal process. During the growth of Fe-G nanosheets, the Co-G precursor began to decompose under the influence of Fe³⁺ ions. The varying decomposition rates on the inner and outer surfaces ultimately led to the formation of the yolk–shell structure. Following this, a layer of polydopamine (PDA) was coated onto the yolk–shell Co-G@Fe-G hollow microspheres, resulting in the formation of Co-G@Fe-G@PDA hollow

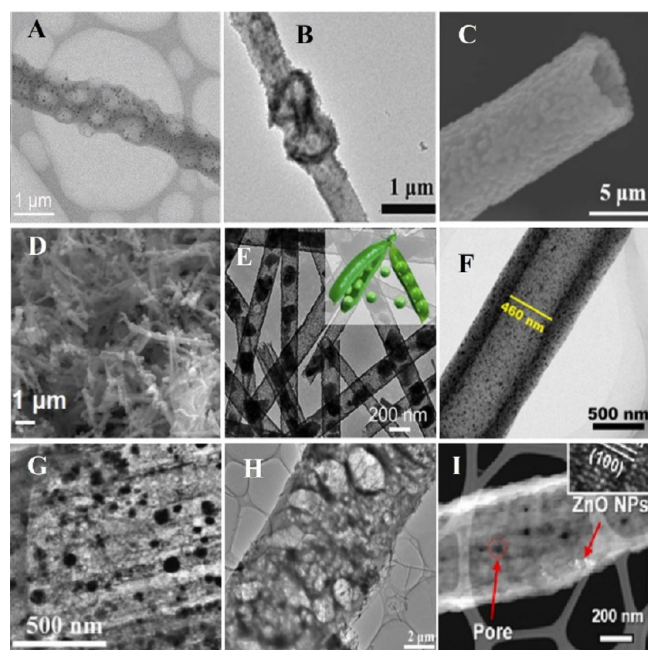


Figure 3. Electron microscope images of hollow nanofibers with modified outer or inner surfaces. (A) TEM image of Fe–N@Ni–HCFs, Open Access.¹⁶ (B) TEM images of Cu/Cu₂O–CF@MoS₂, Reproduced with permission from ref 37. Copyright 2024 Elsevier. (C) The SEM images of PCF7–CFO. Reproduced with permission from ref 38. Copyright 2023 Elsevier. (D) SEM images of N,S–CNFs/Fe₂O₃/Fe₃C/NiCx composites. Reproduced with permission from ref 39. Copyright 2024 American Chemical Society. (E) TEM image of the MoO₃@NiO heterogeneous nanofibers clearly shows that pea-like discrete NPs are wrapped in the thin tube shell. Open Access.⁴¹ (F) TEM images of Fe₃C/HMCs, Reproduced with permission from ref 42. Copyright 2024 American Chemical Society. (G) TEM image of MCCFs–Co/CNTs “tube-in-fiber” structure. Reproduced with permission from ref 43. Copyright 2023 Elsevier. (H) TEM images of fiber parts in Fiber/HNTs/ZIF-67 composite membrane. Reproduced with permission from ref 44. Copyright 2023 Elsevier. (I) HR-TEM images of P–HCNF@ZnO. Reproduced with permission from ref 45. Copyright 2023 Elsevier.

Cu/Cu₂O composite carbon fibers (Cu/Cu₂O–CF@MoS₂) are capable of forming bowknot shape (Figure 3B).³⁷ Yang et al. enhanced one-dimensional phragmites-derived hollow carbon fibers (PCF) by incorporating the soft magnetic material CoFe₂O₄ (CFO). This modification resulted in a distinctive nanofiber structure (PCF7–CFO) featuring uniformly distributed hollow CFO nanospheres on its surface (Figure 3C).³⁸ Similarly, N- and S-doped hollow carbon nanofibers modified simultaneously by Fe₂O₃, Fe₃C, and NiC_x yielded

microspheres. Finally, these Co-G@Fe-G@PDA composites were transformed into $\text{CoS}_2\text{@FeS}_2\text{@NC}$ through in situ carbonization and vulcanization processes (Figure 4A).⁴⁷

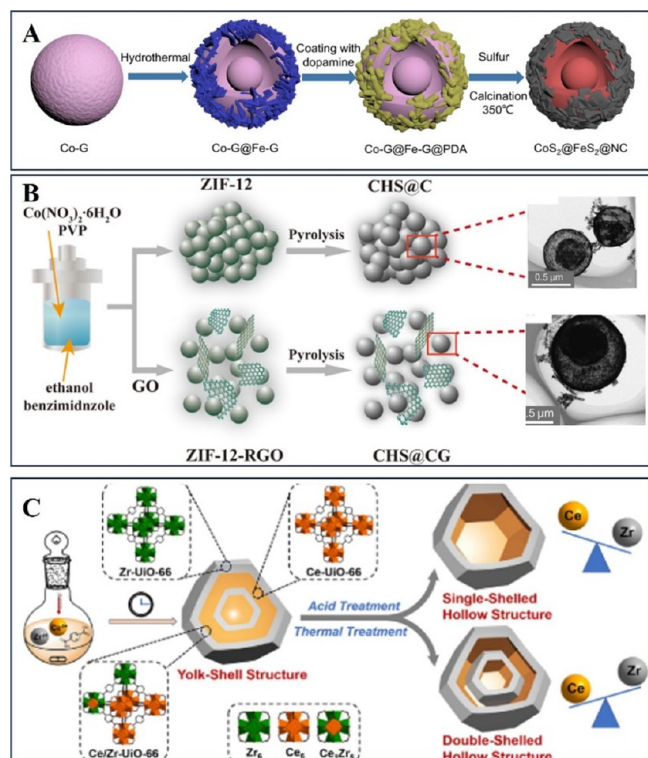


Figure 4. Schematic illustration of the preparation of the yolk-shell structure. (A) Fabrication process of yolk-shell $\text{CoS}_2\text{@FeS}_2\text{@NC}$ hollow microspheres. Reproduced with permission from ref 47. Copyright 2022 Springer Nature. (B) The detailed formation process of two $\text{Co}_3\text{O}_4\text{-C}$ yolk-shell hollow spheres (CHS@C and CHS@CG). Reproduced with permission from ref 49. Copyright 2023 Springer Nature. (C) A “cluster labeling” strategy to construct yolk-shell structures (YSS) with Ce6-UiO-66 as the yolk and Zr6-UiO-66 as the shell, followed by fabrication to single-shelled hollow structures (SSHS) or double-shelled hollow structures (DSHS) through acid or thermal treatments. Reproduced with permission from ref 50. Copyright 2023 American Chemical Society.

Cong et al. synthesized a newly designed Ni-CoO yolk-shell hollow spheres with a diameter of about 500 nm using a step-by-step method, and the Ni-CoO spheres were given a hollow yolk-shell structure by $\text{NH}_3 \cdot \text{H}_2\text{O}$ etching treatment.⁴⁸ Besides, a simple, versatile, and reproducible molecular precursor pyrolysis strategy was proposed for the preparation of yolk-shell hollow nanospheres, which involved the use of ZIF-12 as a pyrolysis precursor to produce two carbon materials, namely CHS@C and CHS@CG . The rapid heat transfer during pyrolysis due to graphene's excellent thermal conductivity enabled the incorporation of graphene to form a bilayer Co_3O_4 yolk-shell hollow sphere structures (Figure 4B).⁴⁹ He et al. posited an innovative engineering tactic termed “cluster labeling” to craft hierarchical porous metal-organic framework (MOF) composites endowed with hollow architectures and adaptable active sites. Through the selective substitution of zirconium within the hexanuclear clusters of UiO-66 with cerium, they induced the creation of nonuniformly dispersed yolk-shell structures. Subsequent acidification or thermal treatment of the yolk-shell structures precursor yielded

singular-shell hollow structures or dual-shell hollow structures correspondingly (Figure 4C).⁵⁰ In addition, the yolk-shell structure Bi_2MoO_6 (YS-BMO) was synthesized by combining excimer blotting and solvothermal methods, with an average diameter of about 1.5 μm .⁵¹ To satisfy practical application requirements, selective functionalization of both the nucleus and shell of yolk-shell structures is essential. This necessitates yolk shells with more intricate structures and compositions. Consequently, further investigation is required to enhance the control over the structure, morphology, and functionality of these yolk-shell nanostructures.

2.3. Multishell Hollow Spherical or Spheroidal-like Structures. Hollow spheres offer advantages over solid NPs due to their higher specific surface area, lower density, and modifiable shells, making them highly beneficial for diverse applications.^{36,52} Hollow spherical or spheroidal-like structures are the most common HNS and have been widely studied in the fields of electrochemistry, environmental pollution, biomaterials, and food. For example, hollow starch NPs were synthesized using a solvent substitution technique combined with gas foaming and salt immersion methods. These NPs exhibited diameters ranging from approximately 30 to 600 nm, with shell thicknesses between 10 and 100 nm, and hollow cores spanning 10 to 500 nm.⁵³ Given the high cost and toxicity of hollow gold NPs, Bhavsar and colleagues synthesized hollow silver NPs using nontoxic and affordable silver compounds as precursors.⁵⁴ Cao and colleagues ingeniously devised a novel nanoenzyme with a distinctive hemispherical structure, achieved by uniformly growing Fe_3O_4 NPs on nitrogen-doped nanohollow carbon spheres.⁵⁵ In addition, Dang et al. proposed a method for forming seed-like hollow metal-organic NPs (SHNPs) using dynamic interfacial-tension-controlled polar growth. In an oil-in-water colloidal emulsion system, DSF nanodroplets interacted with Cpt aqueous solutions. Initially, high interfacial tension maintained the DSF droplet shape, but as DSF and Cpt nucleated, forming DSF-Cpt, the hydrophilicity increased and dynamically adjusted the interfacial tension. This tension guided polar growth and SHNP formation. By varying the DSF solvent's hydrophilicity, DMF volume fraction, DSF to Cpt ratio, and reaction temperature, different SHNP morphologies were achieved (Figure 5A).⁵⁶

In contrast to single-shell structures, multishell hollow structures, comprising two or more shells, are anticipated to exhibit superior performance across diverse domains, including drug delivery, catalysis, and energy storage.⁵⁷ This expectation arises from their enhanced heterogeneity at interfaces and characteristic compartmentalized environments. For example, Liu et al. have introduced a method for crafting hollow nanospheres featuring a double-shell configuration. Specifically, the interior voids were molded by polystyrene spheres (PS), while 3-aminobenzaldehyde resin (APF) served as the nitrogen-doped carbon shell precursor. As shown in Figure 5B, to achieve the double-shell architecture, an intermediate silica shell was interposed between the two APF shells, and subsequent carbonization and silica etching processes ensured the complete separation of the two nitrogen-doped carbon shells derived from APF. Furthermore, to precisely localize ruthenium (Ru) on either the inner (Ru-DSC-I) or outer shell (Ru-DSC-E), Ru^{3+} ions were adsorbed onto the inner and outer APF shells, respectively. A hollow single-shell nano-reactor (Ru-SSC) was also synthesized using a similar method but without adding the second APF shell coating for

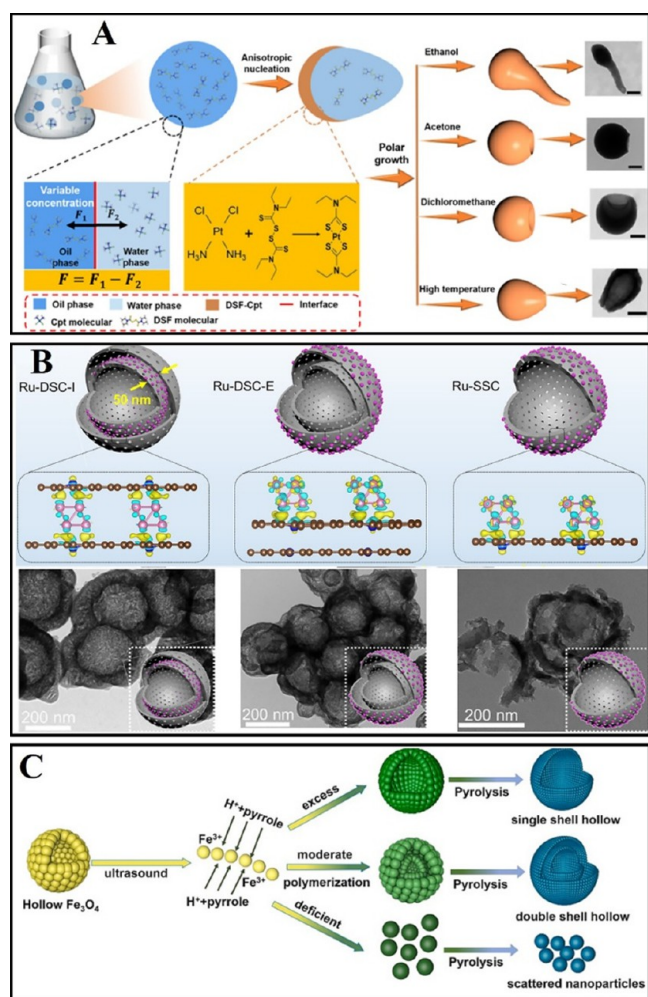


Figure 5. Schematic illustration of the preparation of the spheroidal and multishell spherical structures. (A) Illustration of the polar growth mechanism controlled by the dynamic interfacial tension for synthesizing seed-like hollow NPs with tailored morphologies. Reproduced with permission from ref 56. Copyright 2023 American Chemical Society. (B) Schematic illustration and TEM images of the Ru-SSC, Ru-DSC-I, and Ru-DSC-E. Open access.⁵⁸ (C) Single-shell hollow, double-shell hollow and dispersed spherical particles were formed by modulating the interfacial reaction between hollow Fe_3O_4 nanorods and pyrrolic acid solution, respectively. Reproduced with permission from ref 60. Copyright 2024 Elsevier.

comparison purposes.⁵⁸ Double-shell NiZnOx hollow microspheres for photothermal Enhanced Dynamic Response (EDR) were synthesized using the hard template method, showcasing exceptional catalytic activity and stability.⁵⁹ Double-shell nitrogen-doped carbon hollow particles, derived from polypyrrole, were synthesized through a self-sacrificial template method. The polymerization process was regulated by the interface between the solid and the pyrrolidone acid liquid within the Fe_3O_4 dispersion system, enabling precise control over the carbon micro- and nanostructures (Figure 5C).⁶⁰ Overall, hollow spherical or spheroidal structures are the most widely studied hollow structures. These structures can be precisely and controllably modified to achieve the desired shell composition and morphology using simple and cost-effective methods. Multishell hollow nanostructures, known for their special structures and properties, have found extensive applications in materials chemistry and energy storage.

However, innovative strategies for creating multishell hollow structures are needed in the fields of food and agricultural engineering to bring revolutionary advancements.

2.4. Hollow Polyhedral Structure. Hollow polyhedral structures represent a distinctive class of nanostructures distinguished by their hollow shells comprising multiple facets exhibiting high symmetry and aesthetic appeal. These structures usually consist of multiple facets with hollow interiors, which can be trihedral, cubic, octahedral, and other shapes, and the shells can be composed of different materials or compounds. With the rapid development of synthesis technology, some hollow polyhedral nanostructures have been successfully fabricated using various ingenious methods. As shown in Figure 6A, Liu and his collaborators designed yolk-shelled Sb@Void@GDY nanoboxes. Initially, Cu@Void@GDY nanocages (NCs) were prepared using Cu_2O as the core template and graphdiyne (GDY) as the shell material. The Cu@Void@GDY NCs, serving as both precursor and reductant, were then mixed with SbCl_3 solution for an electrochemical substitution reaction. After the reaction, the products retained the size and wrinkled surface of the original Cu@Void@GDY NCs, while the inner solid metal Cu was transformed into a hollow Sb structure, resulting in the formation of yolk-shelled Sb@Void@GDY nanoboxes.⁶¹ Mu et al. prepared titanium dioxide hollow cubic structures modified with copper and gold NPs using a simple photo-deposition method. This modification enhanced the utilization of visible light and improved the photocatalytic performance of the structures (Figure 6B).⁶² Zhang et al. used MnCO_3 as a template material to create hollow cubic structures. First, they coated cubic MnCO_3 with dopamine (DPA) to form a DPA@MnCO_3 cubic structure, which was then calcined and eroded to produce a hollow cubic structure. Additionally, with the aid of L-cysteine, MnCO_3 induced the surface growth of MoS_2 nanosheets, which were simultaneously converted to MnS . The multihollow HMoS_2 structure was then obtained by selectively dissolving MnS through acid washing. These structures can serve as carriers for *Candida albicans* lipase (CRL) in food ingredient production (Figure 6C).⁶³ In addition, Pan et al. successfully synthesized a novel ZIF-8/ZnS hollow polyhedral heterostructure by sulfurizing ZIF-8 via a solvothermal method. The synthesized samples were used as catalysts for the degradation of AFB1 under UV irradiation. This strategy of coupling MOFs with semiconductors provided a facile method for creating catalysts with enhanced photocatalytic activity, aimed at degrading food contaminants produced by aflatoxins (Figure 6D).⁶⁴

In conclusion, a diverse array of HNS featuring unique geometric configurations and internal cavity architectures has been developed. These nanostructures not only provide expansive surface area and low density but also facilitate the optimization of their performance across diverse applications through meticulous adjustment of shell thickness and morphology. Nonetheless, further exploration is warranted to uncover deeper insights into their synthesis mechanisms and control strategies, aiming for enhanced precision and refinement in structural design. Moreover, varying types of hollow structures pose distinct challenges concerning stability, functionality, and sustainability, necessitating focused endeavors in material design and process refinement.

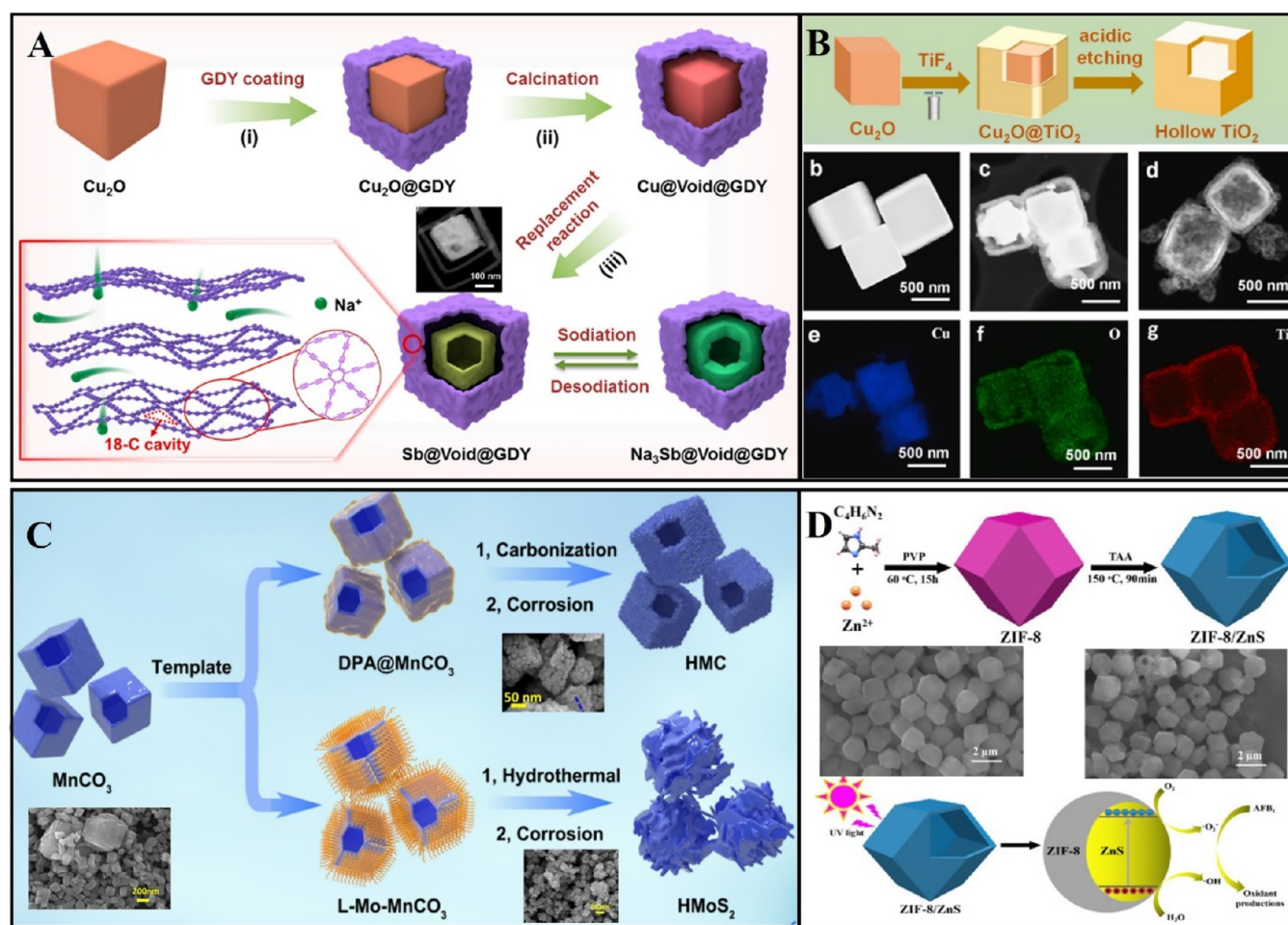


Figure 6. Schematic illustration of the preparation of polyhedral structures. (A) Schematic illustration of Sb@Void@GDY NB preparation. Reproduced with permission from ref 61. Copyright 2023 American Chemical Society. (B) The schematic illustration of the preparation of hollow TiO₂ (a); TEM images (b–d) of Cu₂O, Cu₂O@TiO₂ and TiO₂; TEM elemental mapping images of Cu₂O@TiO₂ (e–g). Reproduced with permission from ref 62. Copyright 2024 Elsevier. (C) Schematic illustration of the process for preparing the hollow mesopore cube supporters. Reproduced with permission from ref 63. Copyright 2023 American Chemical Society. (D) The synthetic route of ZIF-8/ZnS hollow polyhedral heterostructures and photocatalytic degradation pathway of AFB₁ degradation by ZIF-8/ZnS. Reproduced with permission from ref 64. Copyright 2023 Elsevier.

3. UPDATED SYNTHESIS METHODS FOR HNS

To fulfill the needs of both fundamental research and practical applications, it is crucial to synthesize HNS with high homogeneity and structural diversity in a reproducible, scalable, and cost-effective manner. Conventional methods for synthesizing HNS could be categorized into hard template methods (i.e., using rigid nanomaterials such as silica, carbon, or metal NPs to craft templates, followed by coating the templates with a shell material and selectively removing the templates to achieve the hollow structure, and soft template method (i.e., using flexible templates, such as micelles, emulsions, and vesicles, to form the hollow structures through interfacial chemical reactions or self-assembly processes).^{10,14} Since several comprehensive reviews have summarized these synthesis methods, this section will focus on novel approaches developed in the last three years for synthesizing hollow nanostructures. These methods include the solvothermal method, the liquid interfacial assembly method, and the self-templating method.

3.1. The Solvothermal Method. Solvothermal methods can be described as chemical reactions or transformations of precursors within solvents in a confined system at temperatures

exceeding the solvent's boiling point and under elevated pressures. Under supercritical conditions, the increased pressure, high temperatures, and unique behavior of the solvent interact with the precursors in distinctive ways, facilitating the synthesis of the desired material.⁶⁵ Besides, if water is used as the solvent, the method is called "hydrothermal synthesis", which is usually performed below the supercritical temperature of water (374 °C). Recently, a considerable number of HNS have been obtained by solvothermal methods. For example, Liu et al. employed NaMoO₄, CH₄N₂S, and CTAB as precursors, utilizing water as the solvent in a hydrothermal synthesis conducted at 220 °C for 24 h, successfully fabricating hollow micronanospheres of MoS₂.⁶⁶ In addition, Wang et al. synthesized endoexophosphorus (P)-doped hollow spindle-shaped α-Fe₂O₃ NPs via a solvothermal method followed by air calcination. Using FeOOH as the precursor, they demonstrated that varying calcination temperatures influenced the extent of phosphorus doping, thereby transforming the structure from hollow spindle-shaped to solid.¹⁷ Moreover, hollow Fe-MOF NPs⁶⁷ and hollow spherical Mn_{0.5}Zn_{0.5}Fe₂O₄ (MZF-HS) NPs with an average outer diameter of approximately 350 nm and an

average inner diameter of about 220 nm⁶⁸ were prepared by solvothermal methods. In a word, the solvothermal approach for synthesizing novel hollow materials has resulted in a substantial increase in material yield, a significant reduction in costs, and accelerated synthesis times, thereby broadening the applications of solvothermal hollow materials.⁶⁵ Future research utilizing solvothermal synthesis technology holds the potential for more precise control over the size, pore size, and other surface morphologies of synthesized carbon materials, which may enhance their prospects in the energy and biomedical fields.

3.2. Liquid-Interface Assembly Methods. The liquid-interface assembly technique represents a straightforward and adaptable approach for fabricating hollow structures by directly depositing a mesostructured shell layer onto the liquid surface of an emulsion or micelle.¹¹ The efficacy of this strategy hinges on two pivotal factors: first, the creation of numerous droplets or micelles with highly stable interfaces within the reaction medium; and second, the simultaneous assembly of precursors alongside emulsions or micelles at these interfaces. Amphiphilic molecules, such as surfactants and block copolymers, could self-assemble into vesicles or micelles with diverse structures, which can serve as essential structure-directing agents in synthesizing a wide array of functional materials.¹¹ For example, Li et al. fabricated multifunctional nanofibrous hollow microspheres with pore sizes reaching up to tens of micrometers by employing gelatin, mineral oil, and ethanol as raw materials. This synthesis was achieved through the integration of oil/water/oil (O/W/O) double-emulsification technology and thermally induced phase separation.⁵² Starch NPs were prepared by the oil-in-water (O/W) emulsion template method using ethyl acetate as the oil phase and DBS aqueous solution as the water phase. The ethyl acetate in the template was easily and completely removed without affecting the starch shell due to its volatility to form hollow starch NPs.⁶⁹ Li et al. employed the hydrolysis of methyltriethoxysilane under acidic conditions to generate surfactants. These surfactants transformed the system from a suspension to a stable water-in-oil emulsion, facilitating self-assembly into hollow polysiloxane NPs of varying shapes (hollow polysiloxane microspheres (EHMP), apple-shaped hollow polysiloxane particles (AHMP), and bowl-shaped hollow polysiloxane particles (BHMP)) by adjusting the solvent composition.⁷⁰ Additionally, hollow microspheres with controlled mechanical properties and surface morphology were obtained by polymerizing emulsion droplets using silica NPs containing epoxy groups as stabilizers for Pickering emulsions.⁷¹ Similarly, titanium dioxide nanoparticle-stabilized Pickering emulsion could be used to construct molecularly imprinted polymer microspheres with a hollow structure for precise recognition of dibutyl phthalate.⁷² Ma et al. introduce self-assembly method for synthesizing luminescent hollow spherical NPs. Initially, hydrogen-bonded connected micelles (HBCMs) were assembled using poly(styrene-aluminum-hydroxyphenylmaleimide)/poly(4-vinylpyridine) (poly(S-aluminum-HPMI)/P₄VP) interpolymers, which self-assemble into core/shell nanostructures in selective solvents. To fortify the shell structure, two fluorescent compounds, tris(4-bromophenyl) amine (TPA-Br₃) and 1,1,2,2-tetrakis(4-bromophenyl) ethylene (TPE-Br₄), were introduced as cross-linkers. Finally, dimethylformamide (DMF) was utilized to dissolve the core, yielding luminescent hollow spheres.⁷³ Overall, the liquid-interface assembly method expands the

potential for fine-tuning both internal and external structures, allowing for the creation of more complex designs. Nevertheless, given the low thermodynamic stability of the oil or water droplet interface, this method yields limited control over product size, structure, and uniformity.

3.3. The Self-Templating Method. The recently emerging self-templating strategies, including Surface-protected etching, Ostwald ripening, Galvanic replacement, and Kirkendall effect, eliminate the need for presynthesized hard cores and unstable droplets, making it more convenient to produce hollow structures. Generally, the self-templating approach encompasses a biphasic synthesis: (i) the fabrication of template nanomaterials, and (ii) the conversion of the template into a hollow structure.¹¹ In contrast to conventional templating techniques, the templates employed in the self-templating methodology serve not only to establish the internal hollow configuration but also to integrate it into the shell itself. This method boasts several merits, including a relatively straightforward synthesis process, high reproducibility, reduced production costs, and the ability to precisely control shell thickness and particle uniformity. Moreover, the self-templating approach obviates the necessity for heterogeneous coating, thereby facilitating scalability for large-scale production.¹⁴

Surface-protected etching refers to the use of polymer ligands as protective layers to encapsulate solid oxide particles, followed by selective etching of the internal material using appropriate etchants. As shown in Figure 7A, Shao et al. utilized a surface-protected etching method to successfully prepare hollow capsules with a diameter of 500 nm using CaCO₃ NPs, sodium polystyrenesulfonate (PSS), and poly(allylamine hydrochloride) (PAH). During this process, CaCO₃ NPs served as sacrificial templates, with PSS and PAH uniformly coating the surface of CaCO₃ NPs. Subsequently, the CaCO₃ template was dissolved using EDTA·2Na, resulting in hollow capsules with a uniform and stable hollow structure.⁷⁴ Besides, Ostwald ripening is a process involving the dissolution of smaller crystals or sol particles, followed by the redeposition of the dissolved species onto the surfaces of larger crystals or sol particles. As shown in Figure 7B, the Oswald nucleation synthesizes NaBiF₄: Yb, Er (NBFYE) hollow NPs under solvothermal conditions. The NBFYE NPs initially consisted of many smaller crystals; as the reaction time increased, the hollow interior became larger, and the size of the NPs increased slightly. It was attributed to the occurrence of the Ostwald maturation process, in which the energetic nanocrystals located in the central portion dissolve and are redeposited on the outside of the NPs.⁷⁵ The galvanic replacement reaction is considered as an effective self-templating method to prepare HCN with controllable size and shape, porous walls and tunable elemental compositions, especially for noble metals. For example, Sun et al. used cobalt-based nanospheres to synthesize hollow Au nanoshells (hAuNSs) by electrochemical exchange with an outer diameter of 98 nm and a shell thickness of 13 nm (Figure 7C).⁷⁶ The Kirkendall effect is a classical phenomenon in metallurgy that explains the boundary layer motion between two metals due to differences in the diffusion rates of metal atoms. Various HNS formed through the Kirkendall effect, such as the Cu-doped CoP NPs,⁷⁷ Au@Cu₂O,⁷⁸ and hollow PtNi alloy HNS.⁷⁹ As shown in Figure 7D, Wang et al. constructed a stable three-dimensional hollow CoMn₂O₄ nanocage structure via the Kirkendall effect, which not only offered a broader specific

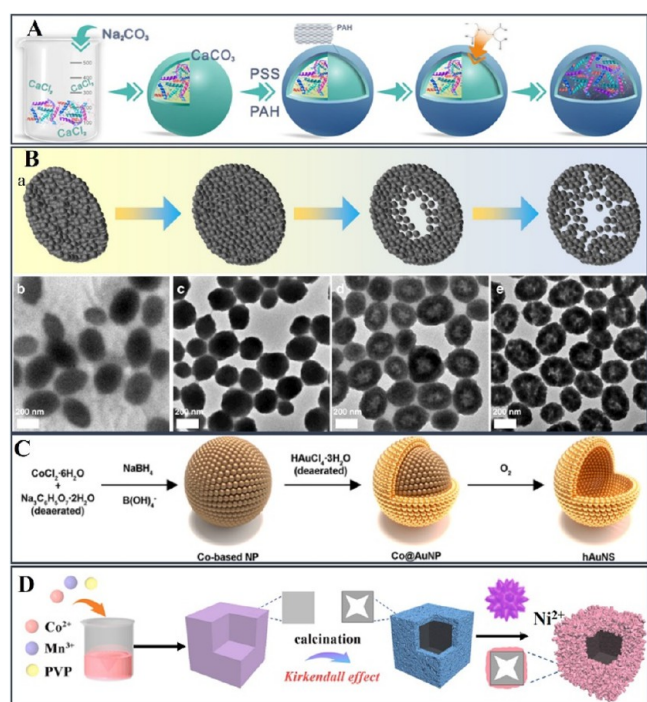


Figure 7. The self-templating strategies for the formation of hollow nanostructures. (A) Schematic diagram of the synthesis of enzyme-loaded SPCs via surface-protected etching method. Open access.⁷⁴ (B) Formation of NaBiF₄:Yb,Er (NBFYE) hollow NPs via Ostwald ripening and their morphological evolution over time. Open Access.⁷⁵ (C) Synthesis of hollow hAuNS NPs by galvanic replacement reaction using Co₂B NPs as sacrificial templates. Reproduced with permission from ref 76. Copyright 2024 American Chemical Society. (D) Synthesis process of CoMn₂O₄@Ni(OH)₂ nanocages via Kirkendall effect. Reproduced with permission from ref 80. Copyright 2024 Elsevier.

surface area and a richer variety of active sites, their porous structure also effectively inhibited the aggregation of NPs and shortened the electron transport distance, resulting in the improvement of the conductivity. Moreover, after the surface growth of worm-like Ni(OH)₂ NPs following hydrothermal growth, the CoMn₂O₄@Ni(OH)₂ nanocage-structured electrochemical sensor was capable of sensitive and rapid detection of trace glucose due to the good synergistic interaction between CoMn₂O₄ and Ni(OH)₂.⁸⁰ Despite the development of numerous synthetic techniques, a universal methodology remains elusive. Thus, a more efficient, environmentally friendly, versatile, and cost-effective synthetic methods still need to pursue.

4. APPLICATIONS OF HNS IN FOOD AND BIOMEDICINE

The structure of hollow NPs plays a crucial role in defining their properties and applications, with each structural variation offering specific advantages and disadvantages. In general, the yolk-shell and multishell hollow structures offer unique benefits in fields such as electromagnetic wave absorption, catalysis, and drug delivery due to their larger void regions between the core and shell providing more surface area and reaction sites.⁸¹ Additionally, hollow nanofibers, nanotubes, and single-shell structures characterized by their higher specific surface area, lower density, and modifiable shells, are especially suitable for food packaging and biosensor applications. These

structures can enhance barrier properties, improve sensitivity in biosensors, and offer versatile functionalization options.^{28,82,83} However, despite their advantages, the synthesis of yolk-shell and multishell hollow structures is often more complex, involving intricate processes that may lead to higher production costs and scalability challenges. These factors can restrict their broader commercial adoption. On the other hand, while the fabrication of hollow nanofibers and single-shell structures may be simpler, achieving uniform size and maintaining structural integrity across large batches remains a significant challenge. In light of these considerations, this section delves into the application of various hollow structures in different domains, particularly focusing on their roles in food packaging, biosensors, and drug delivery, analyzing both their potential benefits and the challenges associated with their structural characteristics.

4.1. Food Packaging. The development of innovative, more sustainable, and environmentally friendly packaging materials to replace traditional plastic packaging materials has been a major focus of research in the food industry.^{8,9} The production of conventional food packaging materials poses significant environmental challenges, as the production process consumes large quantities of water, chemicals, minerals, and oil.⁸ Additionally, it generates heavy metals, wastewater, sludge, and exhaust gases, which can cause environmental degradation.⁸⁴ Hollow nanomaterials, with their distinctive structural attributes, including larger surface areas, high porosity, tunable pore size, and excellent stability, could be easily synthesized through a green approach, offering innovative approaches to address these needs.^{9,85} In addition, HNS can be functionalized using a variety of additives, including antioxidants, antimicrobials, pigments, and fragrances, thereby improving the preservative and sensory properties of packaged foods. For example, Li et al. successfully fabricated thymol-loaded hollow mesoporous silica sphere films by integrating hollow mesoporous silica NPs with zein through an ultrasound-optimized casting method. These films demonstrated exceptional antimicrobial properties and significantly reduced blueberries' water loss and oxidative spoilage (Figure 8A).²³ Besides, a gas phase controlled-release low-density polyethylene film embedded with carvacrol-loaded hollow halloysite nanotubes was also developed. This film demonstrated remarkable antioxidant and antimicrobial activities, showcasing its potential for application in active packaging for solid foods.²⁴ As shown in Figure 8B, Ma et al. have synthesized hollow carbon nanotubes (h-COF)-based hollow NPs by incorporating highly water-soluble amino- (poly(*N*-isopropylacrylamide, PNIPAM) or aldehyde- (methoxy polyethylene aldehyde, PEG-CHO-1000) functionalized polymers into h-COF to form h-COF-g-PNIPAM and h-COF-g-PEG-CHO-1000 NPs. These hollow NPs exhibit excellent water dispersion, high capacity, and responsiveness to thermal stimuli. Notably, the imine-based hollow NPs, with a pore size of 1.3 nm and inner/outer diameters of approximately 150/239 nm, are particularly effective for loading essential oils, thereby prolonging the shelf life of fruits. The storage duration of sage fruits was extended by 4 days compared to the control group without NPs. Furthermore, these hollow NPs are recyclable, demonstrating the potential of COF nanomaterials combined with stimuli-responsive polymers for various food preservation applications.⁸⁶ Considering the thermal instability and wastefulness caused by the sudden release of active substances during food sterilization, Ni et al. fabricated

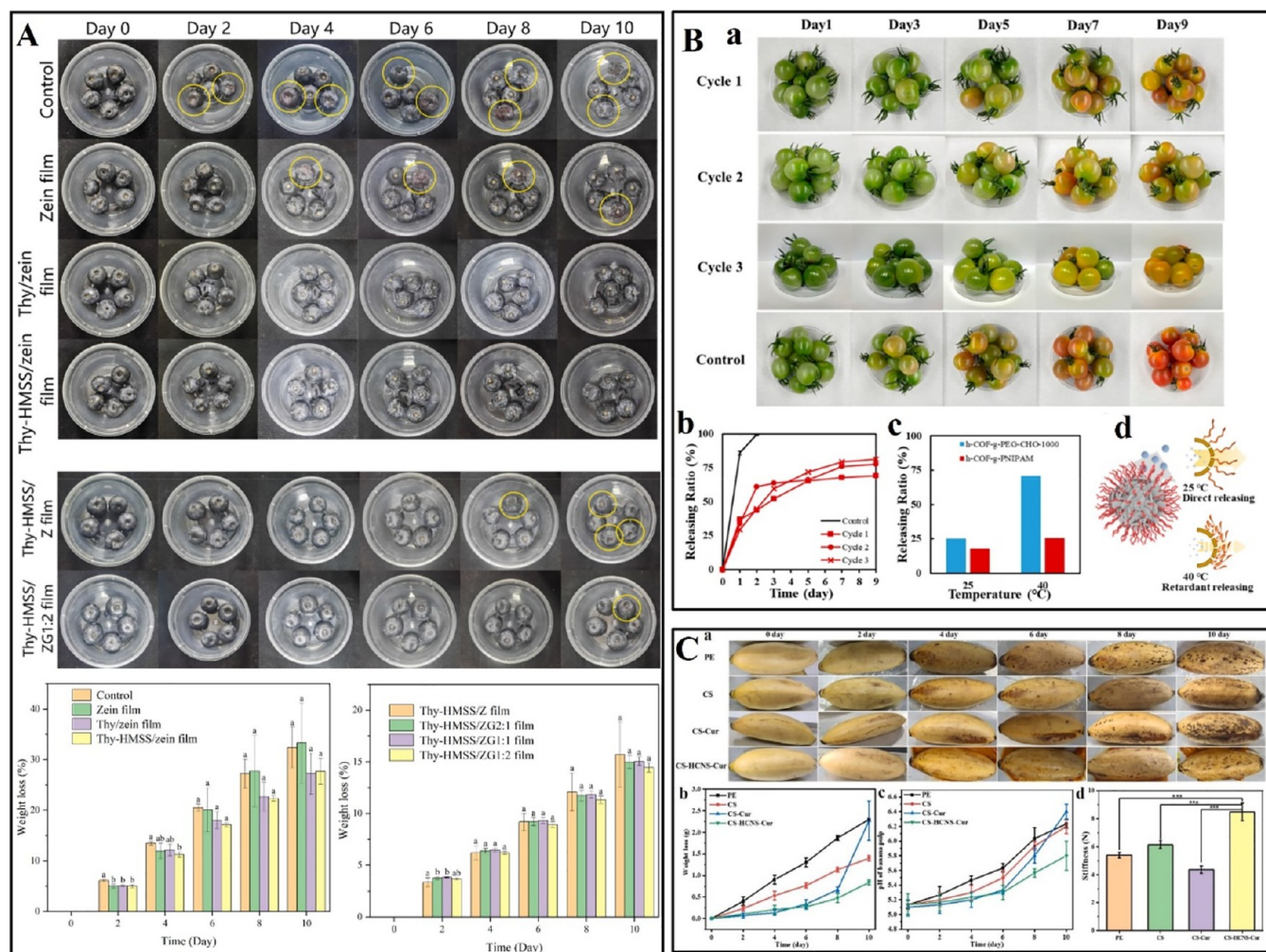


Figure 8. The application of hollow nanostructures in food packing. (A) Blueberry appearance and weight changes during storage in control group, zein film, Thy/zein film, Thy-HMSS/zein film, Thy-HMSS/Z film, and Thy-HMSS/ZG1:2 film. Reproduced with permission from ref 23. Copyright 2024 Elsevier. (B) Ripening process of cherry tomatoes treated with hexanal encapsulated by h-COF-g-PNIPAM, the nanocarriers were recollected and reloaded with hexanal for another two cycles (cycle 2 and 3) of test. The control run using the same amount of hexanal directly was included for comparison (a). Plots of the releasing ratio of hexanal-loaded h-COF-g-PNIPAM against time in three cycles and the control run without using nanocarriers is also included for comparison (b). Releasing ratio of hexanal loaded in h-COF-g-PNIPAM and h-COF-g-PEG-CHO-1000 (c). Schematic illustration of the releasing behaviors of hexanal in h-COF-g-PNIPAM at 25 and 40 °C (d). Reproduced with permission from ref 86. Copyright 2022 American Chemical Society. (C) Experimental results for bananas at different times with various treatments: PE films, chitosan films (CS films), chitosan–curcumin films (CS-Cur films) and chitosan–curcumin loaded hollow g-C₃N₄ films (CS-HCNS-Cur films). (a) Typical pictures of bananas. (b) Weight loss of bananas during storage. (c) The corresponding pH of bananas pulp. (d) Stiffness of bananas on day 10. Reproduced with permission from ref 22. Copyright 2022 Elsevier.

graphitized carbon nitride (g-C₃N₄) into a hollow structure (HCNS) to enhance thermal stability while encapsulating curcumin to prepare (CS-HCNS-Cur) biocomposite film. The film exhibited pH response and slow-release capability to effectively store bananas for up to 10 days (Figure 8C).²²

Furthermore, HNS exhibit the capacity for selective adsorption and desorption of molecules contingent upon their dimensions, morphology, and surface characteristics. Through the discerning extraction of gases such as oxygen, carbon dioxide, moisture, or ethylene, HNS has the potential to enhance the longevity and caliber of packaged food items. For instance, Halloysite nanotubes (HNTs), derived from multilayered nano clay composed of alumina silicates, feature an expansive surface area and a distinctive tubular hollow configuration. These attributes endow packaging materials with enhanced efficacy, including improved physical robustness, mechanical integrity, optical characteristics, thermal and

reheological properties, impermeability to moisture and gases, and heightened active functionality of biopolymers.⁸² Boonsir-iwit et al. engineered a nanocomposite membrane by treating HNTs with an alkaline solution. Notably, the application of a 3% alkaline solution increased the presence of hydroxyl (OH) groups on its surface, thereby enhancing its capacity for ethylene adsorption. The resultant nanocomposite film demonstrated significant efficacy in mitigating weight and firmness deterioration in fresh fruit by impeding ethylene gas infiltration.²¹ Similarly, composite films of CS/HNT were synthesized by incorporating kaolin nanotubes (HNT) into chitosan (CS) via the solution casting technique. These films exhibited enhanced capabilities in UV protection, resistance to water vapor and oxygen permeation, bolstered mechanical resilience, elevated thermal endurance, and proficient ethylene scavenging attributes.²⁰ Overall, the optimal choice of HNS for food packaging materials hinges on the specific requirements of

Table 2. Summarizing the Application of Hollow Nanostructure in the Detection of Substances^a

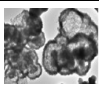
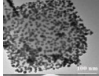
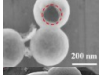
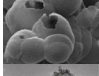
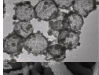
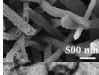
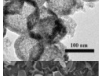

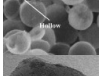
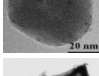
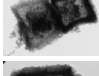

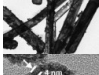
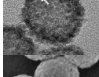
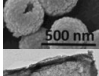
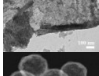
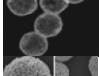
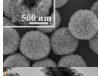
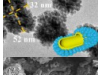

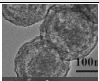
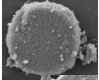
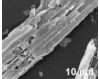
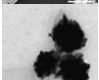
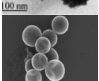
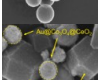
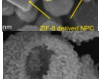
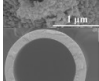
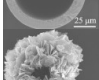
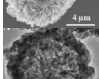
| Hollow core material | Shell modification material | Nanostructure | Detection substance | Liner range | Limit of detection (LOD) | Reference |
|--|--|---|---|---|--|-----------|
| A triple-metal MOF of NiCoFe | Tetracycline antibiotics aptamer |  | Tetracycline (TET) Doxycycline (DOX) Chlortetracycline (CTC) oxytetracycline (OTC) | - | CTC: 5.5 nM TET: 1.3 nM OTC: 1.4 nM DOX: 3.0 nM | 106 |
| Zeolite imidazolate frameworks (ZIFs) | N ₂ and Au NPs |  | MicroRNAs | 0.01–5.0 × 10 ³ fM | 0.04 fM | 107 |
| Nitrogen-doped hollow carbon nanospheres | Au NPs |  | MiR-199a MiR-499 | 0.1–100000 aM | MiR-199a: 0.031 aM MiR-499: 0.027 aM | 108 |
| Nitrogen-doped hollow carbon nanospheres | Progesterone aptamer |  | Progesterone | 10 fM–5.6 μM | 3.33 fM | 109 |
| Hollow manganese silicate nanosphere | - |  | Biothiols | - | 20 nM | 110 |
| Cu (OH) ₂ nanorods with copper foam | Cu ²⁺ , Zn ²⁺ |  | Glucose H ₂ O ₂ | Glucose: 2 μM–3 mM H ₂ O ₂ : 0.8 μM–3.5 mM | 0.17 μM | 96 |
| Hollow metal cerium oxide (CeO ₂ HNPs) | Glucose oxidase |  | β-D-glucose | 1.2 μM–0.8 mM | 1.0 μM | 111 |
| Hollow carbon spheres | Au nanodendrites |  | ultra-trace morphine | 0.01–300 μM | 8.3 nM | 112 |
| Hollow carbon spheres | Pt NPs |  | Listeria monocytogenes | 10–109 CFU mL ⁻¹ | 2 CFU mL ⁻¹ | 29 |
| Hollow Prussian blue with ultra-small silver nanoparticle agents | Glucose oxidase Acetylcholinesterase |  | Glucose (Glu) Trichlorfon (TCF) | Glu: 0.0014–1.0 mM TCF: 2.7 × 10 ⁻⁶ –2.5 μg/mL | Glu: 0.0014 mM TCF: 2.3 pg/mL | 94 |
| Hollow MnO ₂ | Sodium alginate |  | Aspartate aminotransferase (AST), Alanine aminotransferase (ALT), Alkaline phosphatase (ALP). | AST: 5–170 U L ⁻¹ ALT: 5–180 U L ⁻¹ ALP: 5–110 U L ⁻¹ | AST: 4.9 U L ⁻¹ ALT: 3.6 U L ⁻¹ ALP: 0.99 U L ⁻¹ | 113 |
| Hollow ZnNi-MOF | Polypyrrole |  | Norepinephrine bitartrate | 0.1–10 and 10–1000 μM | 0.033 μM | 114 |
| Au/Ag alloy nanotubes | HAuCl ₄ |  | Rhodamine B (RhB) Methylene blue (MB) Malachite green (MG) | RhB: 1.0 × 10 ⁻⁸ –1.0 × 10 ⁻⁴ M MB: 1.0 × 10 ⁻⁹ –1.0 × 10 ⁻⁵ M MG: 1.0 × 10 ⁻⁹ –1.0 × 10 ⁻⁵ M | RhB: 5.3 × 10 ⁻¹¹ M MB: 1.27 × 10 ⁻¹⁰ M MG: 4.07 × 10 ⁻¹² M | 115 |
| Ni NPs | Hollow ruthenium NPs |  | C-reactive protein | 0.12–7.8 ng/mL | 33.2 pg/mL | 90 |
| CeO ₂ hollow spheres | - |  | Ascorbic acid | 1–600 μM 600–3000 μM | 0.33 μM | 93 |
| Hollow CoS ₂ nanotube arrays | Cu NPs |  | Hydrazine in waste water | 1 μM–10 mM | 0.276 μM | 28 |
| hollow carbon-doped nitrogen nanospheres | - |  | Aflatoxin B1 | 0.05–500 ng/mL | 0.023 ng/mL | 116 |
| Hollow TiO ₂ nanospheres | 3-(2-aminoethylamino) propyltrimethoxysilane |  | ppb-level 3-hydroxy-2-butanone biomarker | - | 100 ppb | 117 |
| Au nanorods | AgNO ₃ , H ₂ PtCl ₄ |  | Myoglobin | 0.0001–1000 ng mL ⁻¹ | 0.46 pg mL ⁻¹ | 118 |
| CuMn-PBA nanoboxes | Ni ²⁺ Co ²⁺ |  | Glucose | 0.0005–1 mmol L ⁻¹ and 1–7 mmol L ⁻¹ | 19 nmol L ⁻¹ | 97 |

Table 2. continued

| Hollow core material | Shell modification material | Nanostructure | Detection substance | Linear range | Limit of detection (LOD) | Reference |
|--|---|--|--|--|--|-----------|
| Hollow mesoporous silica NPs | 3-aminopropyltriethoxysilane |  | Free fatty acids in edible oil | 0.2–90 $\mu\text{g g}^{-1}$ | 0.03–0.15 nmol g^{-1} | 119 |
| Ni/Co layered double hydroxide hollow cake | - |  | H_2O_2 in functional beverages | - | 0.22 μM | 120 |
| ZnO/ZnCo ₂ O ₄ hollow tube clusters | - |  | H_2S | 65.38–100 ppm | 30 ppb | 121 |
| Hollow Au@Ag bimetallic nanoflowers | Antigen-mercaptobenzoic acid |  | 2,4-dichlorophenoxyacetic acid | 0.001–100 $\mu\text{g/mL}$ | 0.11 ng/mL | 27 |
| Silver-doped hollow carbon spheres | AgNO_3 |  | Glycated hemoglobin | 0.8–78.4 $\mu\text{g mL}^{-1}$ | 0.35 $\mu\text{g mL}^{-1}$ | 122 |
| ZIF-8 derived NPC | $\text{Au@Co}_3\text{O}_4\text{@CeO}_2$ |  | caffeic acid in food (strawberry and red wine) | 1.0×10^{-9} – 3.0×10^{-6} M | 5.7×10^{-10} M | 91 |
| yolk-shell-structure Bi_2MoO_6 | - |  | ppb-level isopropanol detection | - | 100 ppb | 51 |
| Prussian blue NPs | glucose oxidase micro-particles |  | glucose | 0.1–10 mM | 0.029 mM | 92 |
| $\text{Fe}_3\text{O}_4\text{@MIL-100(Fe)}$ hollow nanoflower | - |  | Benzoylurea insecticides | 0.05–500 ng mL^{-1} | 0.003–0.01 ng mL^{-1} | 123 |
| ZnO-CeO ₂ hollow nanospheres | - |  | Dopamine (DA) Uric Acid (UA) | DA: 5–800 μM UA: 10–1000 μM | DA: 39 μM UA: 0.49 μM | 95 |

^aPBA, Prussian blue analogues; NPC, N-doped carbon nanomaterials.

the application. Typically, hollow nanospheres and nanotubes are preferred due to their high surface area and encapsulation capabilities, which are advantageous for enhancing barrier properties and extending shelf life. Despite the significant benefits that hollow structures offer for food packaging, several challenges remain.^{10,82} In terms of synthesis, many hollow structures are synthesized using complex methods that may not be easily scalable for large-scale production, potentially leading to high costs and limited commercial feasibility. Besides, achieving uniform size and structural integrity across large batches is challenging, as variations in size or shape can affect the performance of the final packaging material. Moreover, ensuring that hollow nanostructures are effectively integrated into the packaging matrix without compromising the material's flexibility, strength, or other desirable properties can be difficult. From a consumer perspective, environmental impact, health concerns, and product cost are critical factors influencing purchasing decisions. Although most materials have been classified as Generally Recognized As Safe (GRAS), there are ongoing safety concerns regarding nanostructured materials, as well as debates about public acceptance of nanotechnology.⁸⁷ Addressing these challenges requires ongoing research and innovation to optimize synthesis methods, enhance material performance, and ensure the safe and sustainable use of hollow nanostructures in food packaging.

4.2. Biosensor. The detection of biomolecules is essential for diagnosing health conditions and identifying contaminants in food. Traditional small molecule detection methods, such as chromatography and spectroscopy, often face inherent

limitations. These include complex sample preparation, lengthy analysis times, costly instrumentation, the need for specialized operators, and limited adaptability to point-of-care devices.⁸⁸ In contrast, biosensors are poised to significantly impact health management due to their convenience and miniaturization.⁸⁹ HNS have expanded their application in biosensors thanks to their high surface area, low density, and versatile surface modification capabilities.^{90,91} Table 2 highlights the recent applications of hollow NPs as biosensors for detecting biomolecules in food products over the past three years.

Biosensors can be categorized into enzyme-based and nonenzyme-based types. Enzyme-based sensors are renowned for their high sensitivity and selectivity. For instance, Zhang et al. utilized glucose oxidase microparticles (GOM), known for their exceptional enzyme stability, along with Prussian blue NPs (PBN), noted for their high enzyme specificity and catalytic activity. These components were employed to modify the inner surface of a polysulfone hollow fiber membrane (PB-GOM@HFM), which enabled effective glucose detection within a linear range of 0.1 to 10 mM, with a limit of detection (LOD) of 0.029 mM (Figure 9A).⁹² In addition, cerium dioxide (CeO_2) hollow nanospheres, as a superoxide dismutase-like nanoenzymes with reversible $\text{Ce}^{3+}/\text{Ce}^{4+}$ redox pairs, could be used to construct a new type of biosensor for the detection of ascorbic acid. The results indicated that in the range of 1 μM –600 μM and 600 μM –3000 μM , the CeO_2 -based photocurrent sensitivity decreased linearly with increasing ascorbic acid concentration, with a detection limit of 0.33 μM .⁹³ Additionally, Hollow Prussian blue with ultrasmall silver

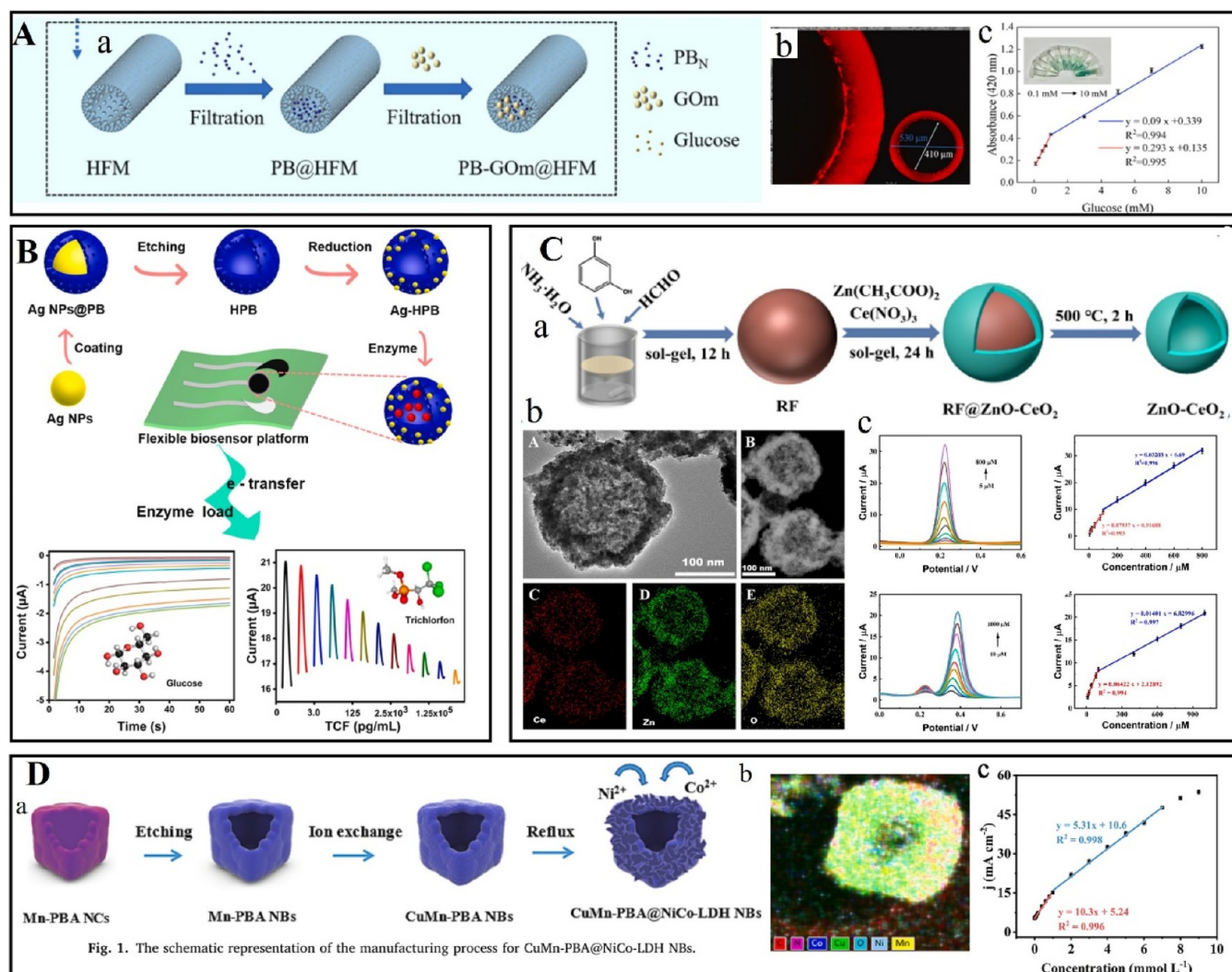


Figure 9. The application of hollow nanostructures in biosensor. (A) Schematic diagram of the fabrication process of PB-GOm@HFM biosensor (a), PB-GOm@HFM dyed with rhodamine B (b), the linear calibration plot for glucose detection and performances of PB-GOx@HFM and PB-GOm@HFM (c). Reproduced with permission from ref 92. Copyright 2023 Elsevier. (B) Schematic diagram of integration of flexible biosensor platform based on Ag-HPB and detection performance of glucose and trichlorfon. Reproduced with permission from ref 94. Copyright 2023 Elsevier. (C) Diagrammatic representation of the synthesis of ZnO-CeO₂ hollow nanospheres (a), TEM and elemental mapping images of ZnO-CeO₂ hollow spheres (b), DPV responses of ZnO-CeO₂/GCE with concentrations of DA and UA in supporting electrolyte solution and corresponding calibration curve (c). Open Access.⁹⁵ (D) The schematic representation of the manufacturing process for CuMn-PBA@NiCo-LDH NBs (a), element distribution of CuMn-PBA@NiCo-LDH NBs (b), amperometric response calibration curve of the sensor at 0.60 V after sequential addition of 1 mmol/L glucose to 0.1 mol/L NaOH (c). Reproduced with permission from ref 97. Copyright 2023 Elsevier.

nanoparticle agents (Ag-HPB) was synthesized by Li et al. (Figure 9B). Modified by glucose oxidase (GOx) and acetylcholinesterase (AChE), the platform demonstrated excellent sensitivity ($24.37 \mu\text{A mM}^{-1} \text{cm}^{-2}$) for glucose (Glu) and LOD of 2.28 pg/mL for trichlorfon (TCF), along with high stability and reproducibility.⁹⁴

Given that enzyme-based sensors are vulnerable to enzyme inactivation caused by factors such as temperature and pH, nonenzymatic sensors have garnered significant attention from researcher due to their lower cost, reproducibility, and less stringent environmental requirements. For example, Yan et al. successfully synthesized ZnO-CeO₂ hollow nanospheres by the hard template method (Figure 9C), where CeO₂ served as a supporting backbone against ZnO agglomeration. Due to the high specific surface area and synergistic effect of ZnO and CeO₂, the excellent detection sensitivities of ZnO-CeO₂ hollow nanospheres for dopamine and uric acid reached

$1122.86 \mu\text{A mM}^{-1} \text{cm}^{-2}$ and $908.53 \mu\text{A mM}^{-1} \text{cm}^{-2}$, respectively, in a neutral environment.⁹⁵ In addition, He et al. prepared three-dimensional hollow CoZn-LDH@CuO nanosheet arrays in situ by growing CoZn-ZIF skeletons on Cu(OH)₂ nanorods using copper foam as precursor. The sensitivities of glucose and H₂O₂ detection were $11,200 (\mu\text{A mM}^{-1} \text{cm}^{-2})$ and $4585 (\mu\text{A mM}^{-1} \text{cm}^{-2})$, respectively, using CoZn-LDH@CuO NSA/CF as the working electrode. The linear ranges were $2 \mu\text{M}$ to 3 mM and $0.8 \mu\text{M}$ to 3.5 mM , respectively, and the detection limit was $0.17 \mu\text{M}$ ($S/N = 3$).⁹⁶ Besides, an integrated electrochemical electrochemical sensor with nanoflowering MoS₂@CuCo₂O₄ heterostructure was constructed for glucose detection. Under optimal conditions, the sensor exhibited a high sensitivity of $1303 \mu\text{A mM}^{-1} \text{cm}^{-2}$ in the range of $0.5\text{--}393.0 \mu\text{mol/L}$ with a low detection limit ($0.5 \mu\text{mol/L}$) and a short response time (2.1 s).⁸⁸ Moreover, Tang et al. constructed Cu-substituted Mn-PBA nanoboxes

Table 3. Summary of the Preparation Methods of Typical Hollow Nanostructures and Their Applications in Drug Delivery over the Last Three Years

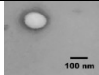
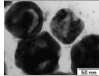
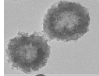
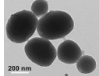
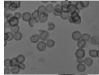
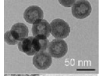
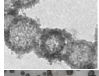
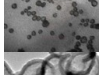
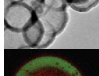
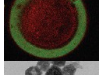
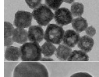
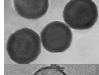
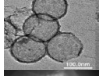
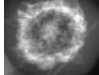
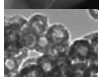
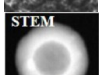
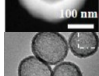
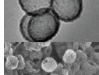
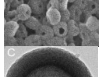
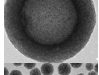
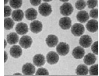
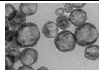
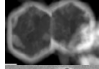
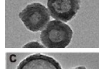
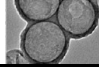
| Preparation method | Hollow core material | Shell modification material | Nanostructure | Delivery ingredient | Reference |
|---|--|---|--|--|-----------|
| Solvent displacement combined with gas-foaming/salt-leaching | NaHCO ₃ | Starch |  | Piroxicam | 53 |
| Sacrificial template method | Ag ₂ O nanoaggregates | Hollow silver NPs |  | Glutathione | 54 |
| Solvothermal method | Hollow Fe-MOF | Hyaluronic acid (HA) |  | Shikonin | 67 |
| Soft template method | Hollow mesoporous silica NPs | Carboxymethyl chitin Glucose-regulated protein 78 binding peptide |  | Doxorubicin (DOX), IL-12 and α-tocopheryl succinate (α-TOS). | 124 |
| Hard template method | Hollow mesoporous silica NPs | Oxidized hyaluronic acid |  | Doxorubicin | 125 |
| Hard template method. | Hollow mesoporous silica NPs | HA |  | Methotrexate Chlorine e6 (Ce6) | 102 |
| The Stober sol-gel method | Hollow MnO ₂ NPs | Disulfide bond |  | Methylene blue (MB) | 126 |
| Galvanic replacement method | Hollow gold NPs | Cancer cell membrane AS1411 aptamer |  | Methotrexate | 103 |
| Template free method | Hollow manganese-doped calcium phosphate NPs | Melanin NPs and Thalidomide |  | Melanin NPs and Thalidomide | 127 |
| Double emulsification combined a thermally induced phase separation | calcium phosphate (CaP) NPs | E7, a short peptide |  | Bone forming peptide | 52 |
| self-templating method | Hollow mesoporous Prussian blue NPs | Bone marrow stromal cell membranes |  | Daunorubicin | 128 |
| The Stober method | Hollow mesoporous silica NPs | S-S bonds and HA |  | Curcumin Chrysin | 32 |
| Sol-gel method | hollow manganese dioxide NPs | Chitosan |  | Resveratrol | 129 |
| Template method | hollow manganese dioxide NPs | polydopamine (PDA) and Cy5.5 |  | Cisplatin | 130 |
| Template method | Hollow barium carbonate NPs | - |  | Methotrexate | 33 |
| Template method | Hollow pollen silica NPs | 4-Carboxyphenylboric acid |  | Pirarubicin | 131 |
| Hard template method | Hollow manganese dioxide | Acrylic acid Allylamine hydrochloride |  | chlorin e6 doxorubicin | 132 |
| Hard template method | PEGylated hollow polydopamine NPs | pPB peptide |  | L-arginin | 104 |
| Self-templating method | Hollow SiO ₂ NPs | Amino-terminated poly (N-vinyl caprolactam) and amino-rich carbon dots |  | Doxorubicin | 133 |
| Self-templating method | Hollow-structured mesoporous silica NPs | - |  | Bcl-2-functional converting peptide (N9) or doxorubicin | 134 |
| Self-templating method | Cu ²⁺ -doped hollow mesoporous polydopamine | PEG-NH ₂ |  | Doxorubicin | 135 |

Table 3. continued

| Preparation method | Hollow core material | Shell modification material | Nanostructure | Delivery ingredient | Reference |
|-----------------------------------|--|--|--|---|-----------|
| Self-templating method | Hollow CuS NPs | Hydroxyapatite Hyaluronic acid |  | doxorubicin hydrochloride | 101 |
| Self-templating method | Hollow Zn-TA NPs | - |  | Tannic acid | 136 |
| Self-templating method | Hollow mesoporous silica nanoparticle | folic acid modified bovine serum albumin |  | methylene blue (MB) and doxorubicin (DOX) | 137 |
| Liquid-interface assembly methods | hollow mesoporous manganese doped silica | lactoferrin |  | Resveratrol | 138 |

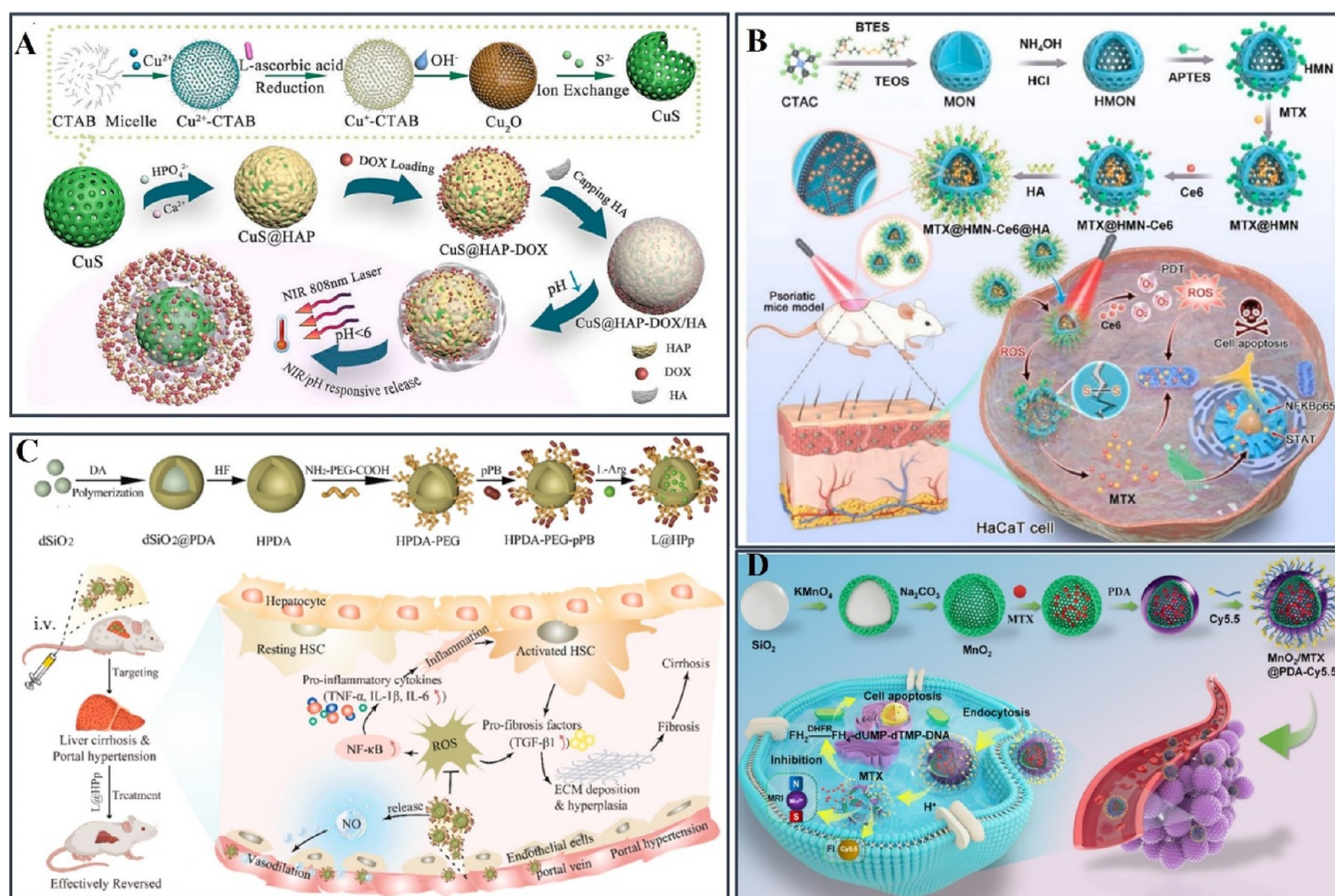


Figure 10. The application of hollow nanostructures in drug delivery. (A) Synthesis procedure of hollow CuS nanoparticle, and schematic illustration of the preparation and dual-stimuli responsive DOX release from CuS@HAP/HA nanoclusters. Reproduced with permission from ref 101. Copyright 2023 Elsevier. (B) Schematic illustration of the preparation of nanomaterials MTX@HMN-Ce6@HA, and increased ROS production of nanomaterials under photodynamic excitation leads to accelerated MTX release of nanomaterials in synergistic psoriasis therapy. Reproduced with permission from ref 102. Copyright 2023 Elsevier. (C) Schematic of the synthesis of L@HPP, and illustration of L@HPP for targeted therapy for liver cirrhosis and portal hypertension. Reproduced with permission from ref 104. Copyright 2023 Elsevier. (D) Schematic illustration of the synthesis and theranostic system of MMPC NPs. Reproduced with permission from ref 105. Copyright 2023 Elsevier.

(CuMn-PBA NBs) using acid etching and cation exchange processes. Subsequently, nickel cobalt aluminate (NiCo-LDH) was deposited on their surfaces by a reflow process to prepare hollow CuMn-PBA@NiCoLDH NBs for the first time (Figure 9D). This unique hollow nanostructure not only stabilized the electrodes by accelerating the redox reaction process of the target molecules, but also increased the surface area and provided multiple active sites. To explore the feasibility of CuMn-PBA@NiCo-LDH NBs/CP for practical applications in

glucose detection, they measured the glucose content in seven real samples, namely, bread, toast, glucose injection, black tea, milk tea, soft drink and soda water, and compared them with those determined by using a glucose kit. The results showed that the electrode achieved a wide linear range (0.0005–1 mmol L⁻¹ and 1–7 mmol L⁻¹) and high sensitivity (10300 μA L/mmol cm⁻² and 5310 μA L/mmol cm⁻²) with a LOD of 19 nmol L⁻¹ under optimal conditions.⁹⁷

4.3. Drug Delivery. Recently, nanotechnology has substantially advanced the development of drug delivery systems. A myriad of delivery carriers with varied structures have been constructed by using metal–organic frameworks (MOFs), proteins, polysaccharides, and liposomes, significantly enhancing the versatility of drug delivery systems.⁹⁸ Among these, hollow NPs have emerged as a prominent candidate for next-generation drug delivery systems due to their unique hollow architecture, high drug loading capacity, controllable release, biocompatibility, and targeting capabilities.^{57,99} To date, advancements in synthesis methods have significantly diversified the composition of hollow nanomaterials, further enhancing their application as drug carriers. Table 3 summarized the applications of hollow nanomaterials prepared by different synthesis methods for drug delivery in the last three years.

More specifically, hollow nanomaterials have a high drug-carrying capacity due to their internal hollow structure, while the multifunctional modification properties of the outer surface makes it susceptible to responding to internal and external stimuli to achieve targeted release.⁹⁹ Bastakoti et al. synthesized hollow BaCO₃ NPs (BC-NPs) featuring a cavity diameter of 15 nm and a shell thickness of 5 nm, utilizing the triblock copolymer poly(ethylene oxide-acrylic acid-styrene) (PEG–PAA-PS) as a template. These hollow BC-NPs with excellent biocompatibility demonstrated effective encapsulation and controlled release of methotrexate.³³ Khan et al. synthesized hollow zein particles utilizing Na₂CO₃ as a sacrificial template, subsequently enhancing these particles with a chitosan coating. This composite particle was investigated for its capacity to encapsulate and safeguard the natural polyphenol resveratrol. The results indicated that the hollow NPs achieved remarkable encapsulation efficiency and loading capacity, reaching 91% and 14%, respectively. The chitosan coating significantly improved both the storage and digestive stability of the resveratrol-loaded hollow zein particles, as well as the storage stability of the encapsulated resveratrol, and demonstrated a sustained *in vitro* release of resveratrol.¹⁰⁰ Due to hyaluronic acid (HA)'s strong affinity for the CD44 protein, it serves as an effective modifier for a diverse array of hollow NPs. For instance, hollow CuS NPs, modified with HA and hydroxyapatite (HAP), demonstrate robust encapsulation and controlled release of doxorubicin hydrochloride (DOX). Notably, they exhibit distinctive dual-responsive characteristics to near-infrared (NIR) and pH stimuli (Figure 10A).¹⁰¹ Furthermore, hollow silica NPs, adorned with HA, adeptly encapsulate both methotrexate (MTX) and chlorin e6 (Ce6), facilitating the photoresponsive release of MTX for treating psoriasis (Figure 10B).¹⁰² Moreover, hollow gold NPs modified by cancer cell membranes and AS1411 could also deliver MTX to realize dual-targeting therapy for colorectal cancer.¹⁰³ In addition, Wang et al. employed pPB peptides to modify polyethylene glycol-coated hollow polydopamine NPs for loading L-arginine (L-Arg). Both *in vitro* and *in vivo* experiments highlighted that these hollow NPs effectively suppressed hepatic fibrosis and targeted hematopoietic stem cells, demonstrating promising clinical potential for treating liver cirrhosis and its complications (Figure 10C).¹⁰⁴ Hollow manganese dioxide NPs modified with dopamine (PDA) and the fluorescent dye Cy5.5 were able to efficiently load methotrexate (MTX) and achieve sustained pH-responsive release, showing significant therapeutic effects on tumors. (Figure 10D).¹⁰⁵ In conclusion,

owing to their distinctive structural characteristics, hollow NPs have emerged as pivotal carriers for drug delivery, marking a significant frontier in modern medicine. As nanotechnology continues to advance and the need for precise drug delivery grows, the utilization of hollow NPs holds great promise in enhancing therapeutic efficacy, reducing side effects, and improving treatment outcomes across various diseases.

5. FUTURE PROSPECTS

Taken together, HNS are versatile and promising materials with various structural forms such as hollow fibers, yolk–shell architectures, multilayered spherical shells, and polyhedral structures. Recent advancements in synthesis methods, including solvothermal methods, liquid-interface assembly, and self-templating techniques, have significantly improved the precision and efficiency of HNS production. Each method offers distinct advantages, facilitating the broadening of applications across various fields. In the food packaging sector, HNS show potential for developing sustainable and eco-friendly alternatives to traditional plastics. These materials not only improve the preservation and sensory properties of packaged foods but also contribute to reducing environmental impact through biodegradability and recyclability. In biosensing applications, HNS can provide high sensitivity and selectivity for detecting biomolecules, thereby enhancing the capabilities of biosensors, which are essential for facilitating health diagnostics and ensuring food safety. Moreover, in drug delivery systems, HNS offer high drug-carrying capacity, precise control over release mechanisms, and targeted delivery capabilities, making them indispensable in advancing therapeutic treatments.

Going forward, significant progress will be made in several key areas of in HNS research and application: (I) Tailored multilayered shells: Advancements in the ability to precisely control the composition and thickness of multiple layers in HNS will be crucial. This could enable more efficient drug delivery systems where the release of therapeutic agents can be finely tuned, or in food packaging where multilayered shells could provide enhanced barrier properties against oxygen, moisture, and other contaminants. (II) Smart and responsive HNS: By tailoring the inner and outer layers of HN to create smart HNS that can respond to external stimuli, such as pH, temperature, or magnetic fields, thereby broadening their potential application areas. (III) Integration into commercial products: For HNS to transition from the laboratory to commercial applications, it is essential to address issues related to stability, reproducibility, safety, and regulatory compliance. On the synthesis side, the use of renewable resources or biodegradable materials for the shell and the development of synthesis processes that minimize waste and energy consumption are important. On the practical application side, collaboration between researchers, industry, and regulatory bodies will be necessary to ensure the safe and effective integration of HNS into consumer products. The continued development and application of hollow NPs hold great promise across various fields. By addressing current challenges and capitalizing on the unique properties of HNS, researchers can unlock new opportunities for innovation and improvement in technology, health, and sustainability.

AUTHOR INFORMATION

Corresponding Author

Zhiyang Du – Jilin Provincial Key Laboratory of Nutrition and Functional Food and College of Food Science and Engineering, Jilin University, Changchun 130062, People's Republic of China; orcid.org/0000-0003-0545-5357; Phone: +86 18686407106; Email: dzy2635@163.com

Authors

Yajuan Li – Jilin Provincial Key Laboratory of Nutrition and Functional Food and College of Food Science and Engineering, Jilin University, Changchun 130062, People's Republic of China

Jingbo Liu – Jilin Provincial Key Laboratory of Nutrition and Functional Food and College of Food Science and Engineering, Jilin University, Changchun 130062, People's Republic of China; orcid.org/0000-0002-1419-0808

David Julian McClements – Department of Food Science, University of Massachusetts, Amherst, Massachusetts 01003, United States

Xin Zhang – Department of Food Science and Engineering, Ningbo University, Ningbo 315211, P.R. China; orcid.org/0000-0002-2073-3338

Ting Zhang – Jilin Provincial Key Laboratory of Nutrition and Functional Food and College of Food Science and Engineering, Jilin University, Changchun 130062, People's Republic of China; orcid.org/0000-0003-4229-6332

Complete contact information is available at:
<https://pubs.acs.org/10.1021/acs.jafc.4c05910>

Notes

The authors declare no competing financial interest.

ACKNOWLEDGMENTS

This work was funded by the National Natural Science Foundation of China (32101941), the National Key R&D Program of China (2022YFD2101002), Jilin University Graduate Innovative Research Project (2024CX149), and Program of China Scholarship Council (202306170154).

REFERENCES

- (1) Junsheng, H.; Mu, Y.; Masud, M. M.; Akhtar, R.; Saif, A. N. M.; Islam, K. M. A.; Hafiz, N. Navigating the nexus: unraveling technological innovation, economic growth, trade openness, ICT, and CO₂ emissions through symmetric and asymmetric analysis. *Humanit Soc. Sci. Commun.* **2024**, *11*, 634.
- (2) Li, G.; Fang, C.; Wang, S.; Sun, S. The Effect of Economic Growth, Urbanization, and Industrialization on Fine Particulate Matter (PM_{2.5}) Concentrations in China. *Environ. Sci. Technol.* **2016**, *50* (21), 11452–11459.
- (3) Pokrajac, L.; Abbas, A.; Chrzanowski, W.; Dias, G. M.; Eggleton, B. J.; Maguire, S.; Maine, E.; Malloy, T.; Nathwani, J.; Nazar, L.; Sips, A.; Sone, J.; van den Berg, A.; Weiss, P. S.; Mitra, S. Nanotechnology for a Sustainable Future: Addressing Global Challenges with the International Network4Sustainable Nanotechnology. *ACS Nano* **2021**, *15* (12), 18608–18623.
- (4) Elzein, B. Nano Revolution: "Tiny tech, big impact: How nanotechnology is driving SDGs progress". *Heliyon*. **2024**, *10* (10), No. e31393.
- (5) Yasun, E.; Gandhi, S.; Choudhury, S.; Mohammadinejad, R.; Benyettou, F.; Gozubenli, N.; Arami, H. Hollow micro and nanostructures for therapeutic and imaging applications. *J. Drug Deliv Sci. Technol.* **2020**, *60*, 102094.
- (6) Sajid, M. Nanomaterials: types, properties, recent advances, and toxicity concerns. *Curr. Opin Environ. Sci. Health.* **2022**, *25*, 100319.
- (7) El-Kady, M. M.; Ansari, I.; Arora, C.; Rai, N.; Soni, S.; Verma, D. K.; Singh, P.; Mahmoud, A. E. D. Nanomaterials: A comprehensive review of applications, toxicity, impact, and fate to environment. *J. Mol. Liq.* **2023**, *370*, 121046.
- (8) Zhao, Z.; Li, Y.; Du, Z. Seafood Waste-Based Materials for Sustainable Food Packing: From Waste to Wealth. *Sustainability*. **2022**, *14* (24), 16579.
- (9) Alizadeh Sani, M.; Khezerlou, A.; McClements, D. J. Zeolitic imidazolate frameworks (ZIFs): Advanced nanostructured materials to enhance the functional performance of food packaging materials. *Adv. Colloid Interface Sci.* **2024**, *327*, 103153.
- (10) Wang, X.; Feng, J.; Bai, Y.; Zhang, Q.; Yin, Y. Synthesis, Properties, and Applications of Hollow Micro-/Nanostructures. *Chem. Rev.* **2016**, *116* (18), 10983–11060.
- (11) Teng, Z.; Li, W.; Tang, Y.; Elzatahry, A.; Lu, G.; Zhao, D. Mesoporous Organosilica Hollow Nanoparticles: Synthesis and Applications. *Adv. Mater.* **2019**, *31* (38), No. e1707612.
- (12) Caruso, F.; Caruso, R. A.; Möhwald, H. Nanoengineering of Inorganic and Hybrid Hollow Spheres by Colloidal Templating. *Science*. **1998**, *282* (5391), 1111–1114.
- (13) Dai, M.; Wang, R. Synthesis and Applications of Nanostructured Hollow Transition Metal Chalcogenides. *Small*. **2021**, *17* (29), No. e2006813.
- (14) Zhu, M.; Tang, J.; Wei, W.; Li, S. Recent progress in the syntheses and applications of multishelled hollow nanostructures. *Mater. Chem. Front.* **2020**, *4* (4), 1105–1149.
- (15) Si, M.; Lin, F.; Ni, H.; Wang, S.; Lu, Y.; Meng, X. Research progress of yolk-shell structured nanoparticles and their application in catalysis. *RSC Adv.* **2023**, *13* (3), 2140–2154.
- (16) Tian, Y.; Wu, Z.; Li, M.; Sun, Q.; Chen, H.; Yuan, D.; Deng, D.; Johannessen, B.; Wang, Y.; Zhong, Y.; Xu, L.; Lu, J.; Zhang, S. Atomic Modulation and Structure Design of Fe-N4Modified Hollow Carbon Fibers with Encapsulated Ni Nanoparticles for Rechargeable Zn-Air Batteries. *Adv. Funct.* **2022**, *32* (52), 202209273.
- (17) Wang, K.; Cao, J.; Gao, J.; Zhao, J.; Jiang, W.; Ahmad, W.; Jiang, J.; Ling, M.; Liang, C.; Chen, J. Unveiling the structure-activity relationship of hollow spindle-like α -Fe₂O₃ nanoparticles via phosphorus doping engineering for enhanced lithium storage. *SM&T*. **2023**, *38*, No. e00744.
- (18) Zhang, L.; Liu, L. L.; Feng, J. J.; Wang, A. J. Methanol-induced assembly and pyrolysis preparation of three-dimensional N-doped interconnected open carbon cages supported FeNb₂O₆ nanoparticles for boosting oxygen reduction reaction and Zn-air battery. *J. Colloid Interface Sci.* **2024**, *661*, 102–112.
- (19) Sun, L.; Lv, H.; Feng, J.; Guselnikova, O.; Wang, Y.; Yamauchi, Y.; Liu, B. Noble-Metal-Based Hollow Mesoporous Nanoparticles: Synthesis Strategies and Applications. *Adv. Mater.* **2022**, *34* (31), No. e2201954.
- (20) Wang, K.; Wu, L.; Li, Y.; Li, H. Preparation and characterization of chitosan/halloysite nanotubes composite film with ethylene scavenging and gas resistance for active food packaging. *Journal of Food Safety*. **2023**, *43* (2), 13027.
- (21) Boonsiriwit, A.; Xiao, Y.; Joung, J.; Kim, M.; Singh, S.; Lee, Y. S. Alkaline halloysite nanotubes/low density polyethylene nanocomposite films with increased ethylene absorption capacity: Applications in cherry tomato packaging. *Food Packag Shelf Life*. **2020**, *25*, 100533.
- (22) Ni, Y.; Nie, H.; Wang, J.; Lin, J.; Wang, Q.; Sun, J.; Zhang, W.; Wang, J. Enhanced functional properties of chitosan films incorporated with curcumin-loaded hollow graphitic carbon nitride nanoparticles for bananas preservation. *Food Chem.* **2022**, *366*, 130539.
- (23) Li, S.; Du, C.; Zhai, M.; Sheng, J.; Song, Y. Enhanced effect of ultrasound and gelatin on physical and antibacterial properties of thymol/hollow mesoporous silicon spheres doped zein film. *Food Biosci.* **2024**, *60*, 104440.
- (24) Lu, L.; Su, Y.; Xu, J.; Ning, H.; Cheng, X.; Lu, L. Development of gas phase controlled-release antimicrobial and antioxidant pack-

aging film containing carvacrol loaded with HNT-4M(halloysite nanotubes etched by 4 mol/L hydrochloric acid). *Food Packag Shelf Life*. **2022**, *31*, 100783.

(25) Dourandish, Z.; Nejad, F. G.; Zaimbashi, R.; Tajik, S.; Askari, M. B.; Salarizadeh, P.; Mohammadi, S. Z.; Oloumi, H.; Mousazadeh, F.; Baghayeri, M.; Beitollahi, H. Recent Advances in Electrochemical Sensing of Anticancer Drug Doxorubicin: A Mini-Review. *Chem. Methodologies* **2024**, *8*, 293–315.

(26) Ding, J.; Zhang, G.; Dai, H.; Chen, H.; Fu, H. Gas sensor preparation based on green biological template: A review. *Sens. Actuator A Phys.* **2024**, *366*, 115051.

(27) Xu, Y.; Kutsanedzie, F. Y. H.; Hassan, M. M.; Zhu, J.; Li, H.; Chen, Q. Functionalized hollow Au@Ag nanoflower SERS matrix for pesticide sensing in food. *Sens. Actuators B Chem.* **2020**, *324*, 128718.

(28) Ou, L.; Yang, J.; Xu, L.; Zhao, S.; Xiong, X.; Xiao, T. Construction of Co-ZIF-derived CoS(2)@Cu hollow heterogeneous nanotube array for the detection of hydrazine in environmental water samples. *Environ. Res.* **2024**, *246*, 118177.

(29) Jiang, X.; Lv, Z.; Rao, C.; Chen, X.; Zhang, Y.; Lin, F. Simple and highly sensitive electrochemical detection of *Listeria monocytogenes* based on aptamer-regulated Pt nanoparticles/hollow carbon spheres nanozyme activity. *Sens. Actuators B Chem.* **2023**, *392*, 133991.

(30) Fazeli-Nasab, B.; Shahraki-Mojahed, L.; Beigomi, Z.; Beigomi, M.; Pahlavan, A. Rapid detection Methods of Pesticides Residues in Vegetable Foods. *Chem. Methodologies* **2022**, *6*, 24–40.

(31) Bahmani, A.; Taghvaei, A.; Firozian, F.; Chehardoli, G. Folic Acid as an Exploiter of Natural Endocytosis Pathways in Drug Delivery. *Chem. Methodologies* **2024**, *8*, 96–122.

(32) Li, Y.; Ertas, Y. N.; Jafari, A.; Taheri, M.; Pilehvar, Y. Co-delivery of curcumin and chrysin through pH-sensitive hyaluronan-modified hollow mesoporous silica nanoparticles for enhanced synergistic anticancer efficiency against thyroid cancer cells. *J. Drug Deliv Sci. Technol.* **2023**, *87*, 104787.

(33) Bastakoti, B. P.; Bhattarai, N.; Ashie, M. D.; Tettey, F.; Yusa, S. I.; Nakashima, K. Single-Micelle-Templated Synthesis of Hollow Barium Carbonate Nanoparticle for Drug Delivery. *Polymers*. **2023**, *15*, 1739.

(34) Park, J. M.; Choi, H. E.; Kudaibergen, D.; Kim, J. H.; Kim, K. S. Recent Advances in Hollow Gold Nanostructures for Biomedical Applications. *Front Chem.* **2021**, *9*, 699284.

(35) Li, L.; Peng, S.; Lee, J. K. Y.; Ji, D.; Srinivasan, M.; Ramakrishna, S. Electrospun hollow nanofibers for advanced secondary batteries. *Nano Energy*. **2017**, *39*, 111–139.

(36) Liu, J.; Liu, X.; Li, D.; Yue, G.; Li, H.; Li, S.; Gao, S.; Wang, N.; Cui, Z.; Bai, J.; Zhao, Y. Multi-Structure Hollow Nanofibers: Controlled Synthesis and Photocatalytic Applications. *ChemNanoMater.* **2020**, *6* (8), 1149–1163.

(37) Zhao, X.; Huang, Y.; Liu, X.; Jiang, H.; Yu, M.; Ma, X.; Zong, M.; Liu, P. Hollow multi-layer bowknot like nanoparticles surface modified by TMDs derived flexible fiber membranes for electromagnetic wave absorption. *Chem. Eng. J.* **2024**, *483*, 149085.

(38) Yang, Y.; Cheng, J.; Pan, F.; Lu, S.; Wang, X.; Cai, L.; Guo, H.; Jiang, H.; Li, L.; Wang, J.; Xiu, Z.; Xu, H.; Lu, W. Phragmites-derived magnetic carbon fiber with hollow assembly architecture toward full-covered effective bandwidth at Ku band. *Carbon*. **2023**, *213*, 118228.

(39) Ge, Y.; Yu, X.; Cao, H.; Yang, X.; Zhao, Y.; Gu, X. N,S-Codoped Hollow Carbon Nanofiber/Multicomponent Nanoparticle Composites for High-Efficiency Lightweight Microwave Absorbers. *ACS Appl. Nano Mater.* **2024**, *7* (8), 9441–9452.

(40) Wang, Y.; Wang, Z.; Sun, H.; Lyu, T.; Ma, X.; Guo, J.; Tian, Y. Multi-Functional Nano-Doped Hollow Fiber from Microfluidics for Sensors and Micromotors. *Biosensors*. **2024**, *14*, 186.

(41) Gao, S.; He, Y.; Yue, G.; Li, H.; Li, S.; Liu, J.; Miao, B.; Bai, J.; Cui, Z.; Wang, N.; Zhang, Q.; Jiang, L.; Zhao, Y. Pea-like MoS₂@NiS_{1.03}-carbon heterostructured hollow nanofibers for high-performance sodium storage. *Carbon Energy*. **2023**, *5* (4), No. e319.

(42) Cheng, J.; Lu, X.; Zhang, D.; Yan, H.; Liu, C.; He, J.; Zheng, C.; Shi, H.; Chu, P. K.; Luo, Y. N-Doped Hollow Multichannel Carbon

Nanofibers Encased in Fe₃C for Lithium-Ion Storage. *ACS Appl. Nano Mater.* **2024**, *7* (9), 10543–10551.

(43) Guan, K.; Yu, Y.; Liu, H.; Luo, J.; Lei, W.; Zhang, H. Design of Co-doped hollow multi-channel carbon fibers for high performance lithium sulfur batteries. *Appl. Surf. Sci.* **2023**, *638*, 157963.

(44) He, Z.; Li, Y.; Liu, G.; Wang, C.; Chang, S.; Hu, J.; Zhang, X.; Vasseghian, Y. Fabrication of a novel hollow wood fiber membrane decorated with halloysite and metal-organic frameworks nanoparticles for sustainable water treatment. *Ind. Crops Prod.* **2023**, *202*, 117082.

(45) Shin, H.-J.; Abbas, S.; Kim, J.; Cho, J.; Ha, H. Y. Near-perfect suppression of Li dendrite growth by novel porous hollow carbon fibers embedded with ZnO nanoparticles as stable and efficient anode for Li metal batteries. *Chemical Engineering Journal*. **2023**, *464*, 142713.

(46) Wang, W.; He, L.; Luo, Q.; Wang, L.; Wang, J.; Chen, H.; Miao, Z.; Yao, Q.; Sun, M. Synthesis and application of core-shell, hollow, yolk-shell multifunctional structure zeolites. *Microporous Mesoporous Mater.* **2023**, *362*, 112766.

(47) Liu, D.; Min, W.; Chen, P.; Xu, D.; Cao, X.; Chen, G.; Wang, R. Facile synthesis of yolk-shell CoS₂@FeS₂@NC hollow microspheres for advanced lithium-ion batteries anode materials. *Ionics*. **2022**, *28* (11), 4967–4976.

(48) Cong, Y.; Ye, L.; Zhang, S.; Zheng, Q.; Zhang, Y.; Lv, S.-W. Efficient degradation of emerging contaminant by newly-constructed Ni-CoO yolk-shell hollow sphere in the presence of peroxymonosulfate: Performance and mechanism. *Process Saf Environ. Prot.* **2023**, *170*, 685–693.

(49) Ding, X.; Ge, X.; Xing, C.; Liu, Y.; Li, T.; Li, X.; Ma, T.; Shen, R.; Liang, E.; Cao, H.; Li, B. Co3O4-C yolk-shell hollow spheres derived from ZIF-12-PVP@GO for superior anode performance in lithium-ion batteries. *J. Mater. Sci.* **2023**, *58* (1), 355–368.

(50) He, H. H.; Yuan, J. P.; Cai, P. Y.; Wang, K. Y.; Feng, L.; Kirchon, A.; Li, J.; Zhang, L. L.; Zhou, H. C.; Fang, Y. Yolk-Shell and Hollow Zr/Ce-UiO-66 for Manipulating Selectivity in Tandem Reactions and Photoreactions. *J. Am. Chem. Soc.* **2023**, *145* (31), 17164–17175.

(51) Zhang, C.; He, X.; Zhou, Y.; Xu, J.; Zheng, Z.; Bian, Y.; Debligny, M. Highly sensitive and stable yolk-shell Bi₂MoO₆ gas sensor for ppb-level isopropanol detection. *Sens. Actuators B Chem.* **2024**, *401*, 135059.

(52) Li, Q.; Ma, C.; Jing, Y.; Liu, X. Multifunctional Nanofibrous Hollow Microspheres for Enhanced Periodontal Bone Regeneration. *Adv. Sci.* **2024**, *11*, No. e2402335.

(53) Belmahdi, L.; Oukacha-Hikem, D.; Makhloufi-Chebli, M. Facile Synthesis of Hollow Starch Nanoparticles for the Delivery of Piroxicam, a Poorly Water-Soluble Drug. *ChemistrySelect*. **2023**, *8* (40), No. e202303116.

(54) Bhavsar, C.; Joshi, R.; Fernandes, T.; Chandramouleeswaran, S.; Khan, T.; Hassan, P. A.; Momin, M.; Ningthoujam, R. S. Glutathione-Capped Hollow Silver Nanoparticles: Optimization of Surface Plasmon Resonance, Photothermal Effect, and In Vitro and In Vivo Biocompatibility. *ACS Appl. Nano Mater.* **2023**, *6* (11), 9276–9289.

(55) Cao, T.; Chen, Z.; Zhang, Y.; Yang, M.; Wang, P. Hemp-ball-like structured Fe₃O₄-hollow carbon sphere nanozymes functionalized carbon fiber cathode for efficient flow-through electro-Fenton. *J. Environ. Chem. Eng.* **2024**, *12* (4), 113097.

(56) Dang, M.; Yu, R.; Han, X.; Shao, L.; Zhao, J.; Ding, Z.; Shi, X.; Zhu, G.; Tao, J.; Mo, J.; Sun, H.; Sun, J.; Luo, W.; Teng, Z. Seed-like Hollow Nanoparticles by a Dynamic Interfacial-Tension-Controlled Polar Growth Strategy. *Chem. Mater.* **2023**, *35* (24), 10542–10549.

(57) Li, Z.; Xu, K.; Qin, L.; Zhao, D.; Yang, N.; Wang, D.; Yang, Y. Hollow Nanomaterials in Advanced Drug Delivery Systems: From Single- to Multiple Shells. *Adv. Mater.* **2023**, *35* (12), No. e2203890.

(58) Liu, X.; Gong, L.; Wang, L.; Chang, C.; Su, P.; Dou, Y.; Dou, S. X.; Li, Y.; Gong, F.; Liu, J. Enabling Ultrafine Ru Nanoparticles with Tunable Electronic Structures via a Double-Shell Hollow Interlayer Confinement Strategy toward Enhanced Hydrogen Evolution Reaction Performance. *Nano Lett.* **2024**, *24* (2), 592–600.

- (59) Li, T.; Tian, Y.; Nginyo, J.; Difuma Luis, D. I.; Cai, W. Light-assisted ethanol dry reforming over NiZnOx hollow microspheres with enhanced activity and stability. *Renew. Energy* **2024**, *227*, 120514.
- (60) Tang, H.; Li, X.; Jin, K.; Shi, Y.; Wang, C.; Guo, W.; Tian, K.; Wang, Y.; Wang, H. Coupling effects of dielectric loss in N-doped carbon double-shelled hollow particles for high-performance microwave absorption. *Appl. Surf. Sci.* **2024**, *653*, 159417.
- (61) Liu, Y.; Qing, Y.; Zhou, B.; Wang, L.; Pu, B.; Zhou, X.; Wang, Y.; Zhang, M.; Bai, J.; Tang, Q.; Yang, W. Yolk-Shell Sb@Void@Graphdiyne Nanoboxes for High-Rate and Long Cycle Life Sodium-Ion Batteries. *ACS Nano* **2023**, *17* (3), 2431–2439.
- (62) Mu, X.; Xu, Q.; Xie, Y.; Ma, Y.; Zhang, Z.; Shen, Z.; Guo, Y.; Yu, J.; Ajmal, S.; Zhang, W.; Zhao, J. Hollow cubic TiO₂ loaded with copper and gold nanoparticles for photocatalytic CO₂ reduction. *J. Alloys Compd.* **2024**, *980*, 173589.
- (63) Zhang, S.; Hou, H.; Zhao, B.; Zhou, Q.; Tang, R.; Chen, L.; Mao, J.; Deng, Q.; Zheng, L.; Shi, J. Hollow Mesoporous Carbon-Based Enzyme Nanoreactor for the Confined and Interfacial Biocatalytic Synthesis of Phytosterol Esters. *J. Agric. Food Chem.* **2023**, *71* (4), 2014–2025.
- (64) Pan, J.; Yang, X.; Zhou, J.; Cheng, W.; Cheng, K. Novel ZIF-8/ZnS hollow polyhedral heterostructures derived from ZIF-8 with enhanced photocatalytic activity for degradation of aflatoxin B1. *Progress in Natural Science: Materials International*. **2023**, *33* (5), 575–580.
- (65) Huo, Y.; Xiu, S.; Meng, L.-Y.; Quan, B. Solvothermal synthesis and applications of micro/nano carbons: A review. *Chem. Eng. J.* **2023**, *451*, 138572.
- (66) Liu, N.; Yu, H.; Liu, Y.; Lin, M.; Lei, Z.; Huang, C.; Qi, F.; Zhou, Y.; Ouyang, X. A novel hierarchical S-scheme heterojunction of 0D/3D Zn_{0.5}Cd_{0.5}S nanoparticles/hollow micro-flower MoS₂ for improved photocatalytic hydrogen evolution. *Appl. Surf. Sci.* **2023**, *632*, 157579.
- (67) Chen, L.; Zhao, D.; Ren, X.; Ren, J.; Meng, X.; Fu, C.; Li, X. Shikonin-Loaded Hollow Fe-MOF Nanoparticles for Enhanced Microwave Thermal Therapy. *ACS Biomater. Sci. Eng.* **2023**, *9* (9), 5405–5417.
- (68) Shen, K.; Li, L.; Tan, F.; Wu, S.; Jin, T.; You, J.; Chee, M. Y.; Yan, Y.; Lew, W. S. Hollow spherical Mn(0.5)Zn(0.5)Fe(2)O(4) nanoparticles with a magnetic vortex configuration for enhanced magnetic hyperthermia efficacy. *Nanoscale*. **2023**, *15* (44), 17946–17955.
- (69) Chang, R.; Cai, W.; Ji, N.; Li, M.; Wang, Y.; Xu, X.; Dai, L.; Xiong, L.; Sun, Q. Fabrication and characterization of hollow starch nanoparticles by heterogeneous crystallization of debranched starch in a nanoemulsion system. *Food Chem.* **2020**, *323*, 126851.
- (70) Li, X.; Zhao, N.; Zhou, C.; Qiao, S.; Wang, J.; Song, S.; Pan, M. Shape-Tunable Hollow Polysiloxane Nanoparticles Based on a Surfactant-Free Soft Templating Method and Their Application as a Drug Carrier. *ACS Appl. Mater. Interfaces*. **2024**, *16* (2), 2672–2682.
- (71) Sun, G.; Cheng, L.; Tong, M.; Chen, L.; Luo, J.; Liu, R. Shrinkage stress of thermal cured epoxy resin reduced by addition of functional hollow microspheres. *Progress in Organic Coatings*. **2023**, *178*, 107466.
- (72) Wang, Z.; Li, Z.; Yan, R.; Wang, G.; Wang, Y.; Zhang, X.; Zhang, Z. Facile fabrication of hollow molecularly imprinted polymer microspheres via pickering emulsion polymerization stabilized with TiO₂ nanoparticles. *Arab. J. Chem.* **2023**, *16* (12), 105304.
- (73) Ma, T.-L.; Du, W.-T.; Gamal Mohamed, M.; Kuo, S.-W. Luminescent hollow spherical nanoparticles with enhanced imaging contrast through hydrogen bonding connected micelles. *Eur. Polym. J.* **2024**, *210*, 112954.
- (74) Shao, Y.; Zhou, Y.; Chen, N.; Xu, W.; Zhou, H.; Lai, W.; Huang, X.; Xiang, X.; Ye, Q.; Zhang, J.; Wang, J.; Parak, W. J.; Wu, Q.; Ding, Y. Synthesizing Submicron Polyelectrolyte Capsules to Boost Enzyme Immobilization and Enhance Enzyme-Based Immunoassays. *ACS Omega*. **2023**, *8* (13), 12393–12403.
- (75) An, R.; Liang, Y.; Deng, R.; Lei, P.; Zhang, H. Hollow nanoparticles synthesized via Ostwald ripening and their upconversion luminescence-mediated Boltzmann thermometry over a wide temperature range. *Light Sci. Appl.* **2022**, *11* (1), 217.
- (76) Sun, D.; Ben Romdhane, F.; Wilson, A.; Salmain, M.; Boujday, S. Hollow Gold Nanoshells for Sensitive 2D Plasmonic Sensors. *ACS Appl. Nano Mater.* **2024**, *7* (5), 5093–5102.
- (77) Wang, X.; Huang, H.; Qian, J.; Li, Y.; Shen, K. Intensified Kirkendall effect assisted construction of double-shell hollow Cu-doped CoP nanoparticles anchored by carbon arrays for water splitting. *Appl. Catal., B* **2023**, *325*, 122295.
- (78) Ivanchenko, M.; Carroll, A. L.; Brothers, A. B.; Jing, H. Facile aqueous synthesis of hollow dual plasmonic hetero-nanostructures with tunable optical responses through nanoscale Kirkendall effects. *Nanoscale Adv.* **2022**, *5* (1), 88–95.
- (79) Byeon, J.-H.; Park, D.-H.; Lee, W.-J.; Kim, M.-H.; Lee, H.-J.; Park, K.-W. Kirkendall effect-driven formation of hollow PtNi alloy nanostructures with enhanced oxygen reduction reaction performance. *J. Power Sources*. **2023**, *556*, 232483.
- (80) Wang, X.; Hao, L.; Du, R.; Wang, H.; Dong, J.; Zhang, Y. Synthesis of unique three-dimensional CoMn₂O₄@Ni(OH)₂ nanocages via Kirkendall effect for non-enzymatic glucose sensing. *J. Colloid Interface Sci.* **2024**, *653*, 730–740.
- (81) Yu, L.; Lan, D.; Guo, Z.; Feng, A.; Wu, G.; Jia, Z.; Feng, X.; Yin, P. Multi-level hollow sphere rich in heterojunctions with dual function: Efficient microwave absorption and antiseptic. *J. Mater. Sci. Technol.* **2024**, *189*, 155–165.
- (82) Deshmukh, R. K.; Kumar, L.; Gaikwad, K. K. Halloysite nanotubes for food packaging application: A review. *Applied Clay Science* **2023**, *234*, 106856.
- (83) Pan, R.; Li, G.; Liu, S.; Zhang, X.; Liu, J.; Su, Z.; Wu, Y. Emerging nanolabels-based immunoassays: Principle and applications in food safety. *TrAC Trends in Analytical Chemistry*. **2021**, *145*, 116462.
- (84) Raul, P. K.; Thakuria, A.; Das, B.; Devi, R. R.; Tiwari, G.; Yellappa, C.; Kamboj, D. V. Carbon Nanostructures As Antibacterials and Active Food-Packaging Materials: A Review. *ACS Omega*. **2022**, *7* (14), 11555–11559.
- (85) Garavand, F.; Khodaei, D.; Mahmud, N.; Islam, J.; Khan, I.; Jafarzadeh, S.; Tahergorabi, R.; Cacciotti, I. Recent progress in using zein nanoparticles-loaded nanocomposites for food packaging applications. *Crit. Rev. Food Sci. Nutr.* **2024**, *64* (12), 3639–3659.
- (86) Ma, Y.; Wang, S.; Zhang, Z.; Cao, X.; Zhang, B.; Wu, D.; Chen, K.; Wang, W. J.; Liu, P. Grafting Hollow Covalent Organic Framework Nanoparticles with Thermal-Responsive Polymers for the Controlled Release of Preservatives. *ACS Appl. Mater. Interfaces*. **2022**, *14*, 22982–22988.
- (87) Jafarzadeh, S.; Forough, M.; Kouzegaran, V. J.; Zargar, M.; Garavand, F.; Azizi-Lalabadi, M.; Abdollahi, M.; Jafari, S. M. Improving the functionality of biodegradable food packaging materials via porous nanomaterials. *Compr. Rev. Food Sci. Food Saf.* **2023**, *22* (4), 2850–2886.
- (88) Wang, H.; Zhu, W.; Xu, T.; Zhang, Y.; Tian, Y.; Liu, X.; Wang, J.; Ma, M. An integrated nanoflower-like MoS(2)@CuCo(2)O(4) heterostructure for boosting electrochemical glucose sensing in beverage. *Food Chem.* **2022**, *396*, 133630.
- (89) Cao, W.; Guo, T.; Wang, J.; Xu, G.; Jiang, J.; Liu, D. Cu-based materials: Design strategies (hollow, core-shell, and LDH), sensing performance optimization, and applications in small molecule detection. *Coord. Chem. Rev.* **2023**, *497*, 215450.
- (90) Son, S. E.; Gupta, P. K.; Hur, W.; Lee, H. B.; Han, D. K.; Seong, G. H. Hollow Ruthenium Nanoparticles with Enhanced Catalytic Activity for Colorimetric Detection of C-Reactive Protein. *ACS Appl. Nano Mater.* **2023**, *6* (13), 11435–11442.
- (91) Yang, Y.; Li, J.; Wang, Y.; Liu, Z.; Xie, Y.; Zhao, P.; Hu, X.; Fei, J. ZIF-derived porous carbon loaded multicomponent heterostructured yolk@shell nanospheres as an ultrasensitive electrochemical sensing platform for the detection of caffeic acid in food. *Electrochim. Acta* **2024**, *486*, 144147.
- (92) Zhang, C.; Wei, C.; Chen, D.; Xu, Z.; Huang, X. Construction of inorganic-organic cascade enzymes biosensor based on gradient

polysulfone hollow fiber membrane for glucose detection. *Sens. Actuators B Chem.* **2023**, 385, 133630.

(93) Mao, A.; Zhang, Y.; Xu, Q.; Li, J.; Li, H. Superoxide dismutase-like cerium dioxide hollow sphere-based highly specific photo-electrochemical biosensing for ascorbic acid. *Talanta*. **2024**, 269, 125472.

(94) Li, R.; Zhang, W.; Meng, F.; Li, X.; Li, Z.; Fang, Y.; Zhang, M. Hollow Prussian blue with ultrafine silver nanoparticle agents (Ag-HPB) integrated sensitive and flexible biosensing platform with highly enzyme loading capability. *Talanta*. **2024**, 266, 125036.

(95) Zhang, Y.; Yan, X.; Chen, Y.; Deng, D.; He, H.; Lei, Y.; Luo, L. ZnO-CeO₂ Hollow Nanospheres for Selective Determination of Dopamine and Uric Acid. *Molecules*. **2024**, 29 (8), 1786.

(96) He, Z.; Jin, Y.; Yuan, X.; Xue, K.; Hu, J.; Xiong, X. ZIF in situ transformation hollow porous self-supporting CoZn-LDH@CuO electrode for electrochemical sensing of glucose and H₂O₂. *Microchemical Journal*. **2023**, 195, 109457.

(97) Tang, X.; Yuan, X.; Jin, Y.; Wu, J.; Ling, C.; Huang, K.; Zhu, L.; Xiong, X. A novel hollow CuMn-PBA@NiCo-LDH nanobox for efficient detection of glucose in food. *Food Chem.* **2024**, 438, 137969.

(98) Ezike, T. C.; Okpala, U. S.; Onoja, U. L.; Nwike, C. P.; Ezeako, E. C.; Okpara, O. J.; Okoroafor, C. C.; Eze, S. C.; Kalu, O. L.; Odoh, E. C.; Nwadike, U. G.; Ogbodo, J. O.; Umeh, B. U.; Ossai, E. C.; Nwanguma, B. C. Advances in drug delivery systems, challenges and future directions. *Heliyon*. **2023**, 9 (6), No. e17488.

(99) Zhao, D.; Wei, Y.; Xiong, J.; Gao, C.; Wang, D. Response and Regulation of the Microenvironment Based on Hollow Structured Drug Delivery Systems. *Adv. Funct.* **2023**, 33 (31), 2300681.

(100) Khan, M. A.; Chen, L.; Liang, L. Improvement in storage stability and resveratrol retention by fabrication of hollow zein-chitosan composite particles. *Food Hydrocolloids*. **2021**, 113, 106477.

(101) Yang, P.; Chen, W.; Li, J.; Cao, S.; Bi, X.; Shi, J. Hollow CuS nanoparticles equipped with hydroxyapatite/hyaluronic acid coating for NIR/pH dual-responsive drug delivery. *Int. J. Biol. Macromol.* **2023**, 253, 127150.

(102) Fan, Z.; Zhao, G.; Gan, Y.; Wei, L.; Xia, R.; Lu, M.; Wang, Z. Synergistic chemo-photodynamic therapy based on hollow mesoporous organosilica nanoparticles for reducing psoriasis-like inflammation. *Chem. Eng. J.* **2024**, 490, 151613.

(103) Hassibian, S.; Taghdisi, S. M.; Jamshidi, Z.; Samie, A.; Alinezhad Nameghi, M.; Shayan, M.; Farrokhi, N.; Alibolandi, M.; Ramezani, M.; Dehnavi, S. M.; Abnous, K. Surface modification of hollow gold nanoparticles conducted by incorporating cancer cell membrane and AS1411 aptamer, aiming to achieve a dual-targeted therapy for colorectal cancer. *Int. J. Pharm.* **2024**, 655, 124036.

(104) Wang, Y.; Liu, Y.; Liu, Y.; Zhong, J.; Wang, J.; Sun, L.; Yu, L.; Wang, Y.; Li, Q.; Jin, W.; Yan, Z. Remodeling liver microenvironment by L-arginine loaded hollow polydopamine nanoparticles for liver cirrhosis treatment. *Biomaterials*. **2023**, 295, 122028.

(105) Liu, J.; Li, C.; Xie, Z.; Jia, Q.; Guo, C.; Wang, Z.; Wu, S.; Li, F.; Li, Z.; Hao, L. Hollow Manganese Dioxide Nanoparticles for Drug Delivery and Imaging. *ACS Appl. Nano Mater.* **2024**, 7 (11), 13557–13567.

(106) Chen, Q.; Zhang, H.; Sun, H.; Yang, Y.; Zhang, D.; Li, X.; Han, L.; Wang, G.; Zhang, Y. Sensitive dual-signal detection and effective removal of tetracycline antibiotics in honey based on a hollow triple-metal organic framework nanozymes. *Food Chem.* **2024**, 442, 138383.

(107) Gao, Y.-p.; Huang, K.-j.; Hou, Y.-y.; Wang, B.-y.; Xu, Q.; Shuai, H.; Xu, J.; Li, G. Nitrogen-doped dodecahedral hollow carbon combined with amplification strategy to construct ultra-sensitive self-powered biosensor for highly stable and real-time monitoring microRNA. *Sens. Actuators B Chem.* **2023**, 387, 133816.

(108) Gao, Y. P.; Huang, K. J.; Wang, B. Y.; Xu, Q.; Shuai, H.; Li, G. Constructed a self-powered sensing platform based on nitrogen-doped hollow carbon nanospheres for ultra-sensitive detection and real-time tracking of double markers. *Anal. Chim. Acta* **2023**, 1267, 341333.

(109) Ghanbarzadeh, M.; Ghaffarinejad, A.; Shahdost-Fard, F. A nitrogen-doped hollow carbon nanospheres-based aptasensor for non-invasive salivary detection of progesterone. *Talanta*. **2024**, 273, 125927.

(110) Han, M.; Huang, J.; Niu, Z.; Guo, Y.; Wei, Z.; Ding, Y.; Li, C.; Wang, P.; Wen, G.; Li, X. Amorphous hollow manganese silicate nanosphere oxidase mimic for ultrasensitive and high-reliable colorimetric detection of biothiols. *Mikrochim. Acta* **2023**, 190 (11), 450.

(111) Huang, C.; Cheng, Y.; Zhang, Y.; Zhao, K.; Liu, H.; Zhang, B.; Cao, J.; Xu, J.; Liu, J. A molecularly imprinted sensing system for specific detection of monosaccharides based on CeO₂ hollow nanosphere cascade enzyme system. *Sens. Actuators B Chem.* **2023**, 379, 133222.

(112) Imanzadeh, H.; Khataee, A.; Hazraty, L.; Amiri, M. Broken hollow carbon spheres decorated by gold nanodendrites as the advanced electrochemical sensing platform for sensitive tracing of morphine in human serum and saliva. *Sens. Actuators B Chem.* **2024**, 398, 134738.

(113) Li, S.; Chen, Z.; Yang, F.; Yue, W. Self-template sacrifice and in situ oxidation of a constructed hollow MnO₂ nanozymes for smartphone-assisted colorimetric detection of liver function biomarkers. *Anal. Chim. Acta* **2023**, 1278, 341744.

(114) Liu, J.; Sun, W.; Zha, X.; Sun, G.; Wang, Y. A novel hollow nanostructure with charge collection function based on bimetallic MOFs: Ameliorating the catalytic reaction of norepinephrine bitartrate in serum. *Colloids Surf. A Physicochem. Eng. Asp.* **2023**, 677, 132419.

(115) Liu, Y.-l.; Zhu, J.; Weng, G.-j.; Li, J.-j.; Zhao, J.-w. Simultaneous determination of three food contaminants in shrimp paste by hollow porous pentagonal Au/Ag alloy nanotubes with excellent SERS activity. *Sens. Actuators B Chem.* **2022**, 373, 132766.

(116) Qiao, M.; Wan, Z.; Wang, X.; Suo, Z.; Liu, Y.; Wei, M. A novel fluorescent aptasensor based on H-shaped DNA nanostructure and hollow carbon-doped nitrogen nanospheres for sensitive detection of AFB1. *Food Control*. **2024**, 162, 110430.

(117) Sun, S.; Zhao, C.; Zhang, Z.; Wang, D.; Yin, X.; Han, J.; Wei, J.; Zhao, Y.; Zhu, Y. Highly selective QCM sensor based on functionalized hierarchical hollow TiO₂ nanospheres for detecting ppb-level 3-hydroxy-2-butanone biomarker at room temperature. *Chin. Chem. Lett.* **2024**, 109939.

(118) Tang, C.; Wang, A. J.; Feng, J. J.; Cheang, T. Y. Mulberry-like porous-hollow AuPtAg nanorods for electrochemical immunosensing of biomarker myoglobin. *Mikrochim. Acta* **2023**, 190 (6), 233.

(119) Wang, Y.; Yang, C.; Wang, X.; Zhang, S.; Wang, S.; Wu, D.; Rakariyatham, K.; Hu, J.; Zhao, Q. Determination of free fatty acids in edible oil based on hollow mesoporous silica nanoparticles. *Food Chem.* **2024**, 443, 138561.

(120) Wu, Y.; Xu, F.; Wu, C.; Hu, K.; Yang, Q.; Huang, K. Preparation of Ni/Co layered double hydroxide hollow cakes as an electrochemical sensing platform for monitoring the production of hydrogen peroxide in formulated beverages. *Microchem. J.* **2024**, 202, 110793.

(121) Xu, T.; Zhao, J.; Zhao, F.; Cong, W.; Wang, G. Synthesis of ZnO/ZnCo₂O₄ hollow tube clusters by a template method for high-sensitive H₂S sensor. *Sens. Actuators B Chem.* **2023**, 394, 134338.

(122) Yang, Y.; Dong, H.; Yin, H.; Gu, J.; Zhang, Y.; Xu, M.; Wang, X.; Zhou, Y. Controllable preparation of silver-doped hollow carbon spheres and its application as electrochemical probes for determination of glycated hemoglobin. *Bioelectrochemistry*. **2023**, 152, 108450.

(123) Zhang, N.; Mu, M.; Zhu, S.; Gao, Y.; Lu, M. Well-defined Fe₃O₄@MIL-100(Fe) hollow nanoflower heterostructures for selective detection and monitoring of benzoyleurea insecticides from food and water. *Food Chem.* **2024**, 435, 137579.

(124) Ding, X.; Liu, X.; Qiu, T.; Zhou, Y.; Michal, N.; Roman, S.; Liu, Q.; Liu, Y.; Peng, N. Modulation of macrophage polarity with carboxymethyl chitin gated hollow mesoporous silica nanoparticles for elevating anti-tumor chemotherapy. *Int. J. Biol. Macromol.* **2024**, 261, 129761.

- (125) Enyu, X.; Xinbo, L.; Xuelian, C.; Huimin, C.; Yin, C.; Yan, C. Construction and performance evaluation of pH-responsive oxidized hyaluronic acid hollow mesoporous silica nanoparticles. *Int. J. Biol. Macromol.* **2024**, *257*, 128656.
- (126) Hao, C.; Shao, Y.; Tian, J.; Song, J.; Song, F. Dual-Responsive hollow mesoporous organosilicon nanocarriers for photodynamic therapy. *J. Colloid Interface Sci.* **2024**, *659*, 582–593.
- (127) Li, J.; Qu, B.; Wang, Q.; Ning, X.; Ren, S.; Liu, C.; Zhang, R. Hollow Manganese-Doped Calcium Phosphate Nanoparticles Treated with Melanin Nanoparticles and Thalidomide for Photothermal and Anti-angiogenic Cancer Therapy. *ACS Appl. Nano Mater.* **2022**, *5* (6), 7733–7743.
- (128) Li, Q.-Q.; Wang, F.; Bai, H.-Y.; Cui, Y.; Ma, M.; Zhang, Y. Hollow Mesoporous Prussian Blue Nanoparticles Loaded with Daunorubicin for Acute Myeloid Leukemia Treatment. *ACS Appl. Nano Mater.* **2023**, *6* (23), 22128–22141.
- (129) Li, Y.; Zou, Z.; An, J.; Wu, Q.; Tong, L.; Mei, X.; Tian, H.; Wu, C. Chitosan-modified hollow manganese dioxide nanoparticles loaded with resveratrol for the treatment of spinal cord injury. *Drug Delivery* **2022**, *29* (1), 2498–2512.
- (130) Liu, J.; Guo, C.; Li, C.; Jia, Q.; Xie, Z.; Wang, Z.; Tian, H.; Li, Z.; Hao, L. Redox/pH-responsive hollow manganese dioxide nanoparticles for thyroid cancer treatment. *Front Chem.* **2023**, *11*, 1249472.
- (131) Wang, L.; Qi, F.; Bi, L.; Yan, J.; Han, X.; Wang, Y.; Song, P.; Wang, Y.; Zhang, H. Targeted hollow pollen silica nanoparticles for enhanced intravesical therapy of bladder cancer. *Biomater. Sci.* **2023**, *11* (14), 4948–4959.
- (132) Wang, W.; Chen, X.; Li, J.; Jin, Q.; Jin, H. J.; Li, X. Hollow MnO₂ Nanoparticles Loaded with Functional Genes as Nanovaccines for Synergistic Cancer Therapy. *ACS Appl. Nano Mater.* **2022**, *5* (8), 10537–10547.
- (133) Wu, S.; Shi, J.; Chen, X.; Bai, L.; Wu, Q.; Zhang, G. Endogenous NO-release multi-responsive hollow mesoporous silica nanoparticles for drug encapsulation and delivery. *Colloids Surf. B Biointerfaces.* **2023**, *227*, 113346.
- (134) Wu, Y.; Ma, F.; Yu, L.; Lin, R.; Lin, S.; Guo, Z.; Zhou, M.; Li, M.; Zhang, Y.; Xie, J. Unique Advantages of Dendrimers-Structured Mesoporous Silica Nanoparticles over Traditional Hollow Ones in Delivering Bcl2-Functional Converting Peptide for Multidrug Resistant Cancer Treatment. *Adv. Healthc. Mater.* **2024**, No. e2400888.
- (135) Xu, Q.; Li, J.; Liu, B.; Chen, G.; Qi, W.; Lu, J.; Wang, S.; Zhao, Q. Biodegradable copper-doped hollow mesoporous polydopamine nanoparticles for chemo/photothermal/chemodynamic synergistic therapy. *J. Drug Deliv. Sci. Technol.* **2023**, *89*, 105015.
- (136) Zhang, C.; Li, Q.; Xing, J.; Yang, Y.; Zhu, M.; Lin, L.; Yu, Y.; Cai, X.; Wang, X. Tannic acid and zinc ion coordination of nanase for the treatment of inflammatory bowel disease by promoting mucosal repair and removing reactive oxygen and nitrogen species. *Acta Biomater.* **2024**, *177*, 347–360.
- (137) Zhang, Y.; Ye, Z.; He, R.; Li, Y.; Xiong, B.; Yi, M.; Chen, Y.; Liu, J.; Lu, B. Bovine serum albumin-based and dual-responsive targeted hollow mesoporous silica nanoparticles for breast cancer therapy. *Colloids Surf., B* **2023**, *224*, 113201.
- (138) Zou, Z.; Wen, S.; Li, Y.; An, J.; Wu, Q.; Tong, L.; Mei, X.; Tian, H.; Wu, C. Novel lactoferrin-functionalized manganese-doped silica hollow mesoporous nanoparticles loaded with resveratrol for the treatment of ischemic stroke. *Mater. Today Adv.* **2022**, *15*, 100262.